



**Boronate affinity materials for separation and molecular recognition: structure, properties and applications**

Journal:	<i>Chemical Society Reviews</i>
Manuscript ID:	CS-SYN-01-2015-000013.R2
Article Type:	Review Article
Date Submitted by the Author:	23-Aug-2015
Complete List of Authors:	Li, Daojin; Nanjing University, School of Chemistry and Chemical Engineering Chen, Yang; Nanjing University, School of Chemistry and Chemical Engineering Liu, Zhen; Nanjing University, School of Chemistry and Chemical Engineering

Cite this: DOI: 10.1039/c0xx00000x

www.rsc.org/xxxxxx

ARTICLE TYPE

# Boronate affinity materials for separation and molecular recognition: structure, properties and applications

Daojin Li, Yang Chen, Zhen Liu\*

Received (in XXX, XXX) Xth XXXXXXXXX 20XX, Accepted Xth XXXXXXXXX 20XX

DOI: 10.1039/b000000x

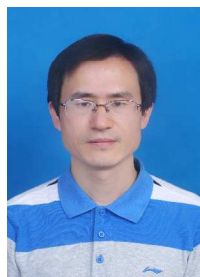
Boronate affinity materials, as unique sorbents, have emerged as important media for the selective separation and molecular recognition of *cis*-diol-containing compounds. With the introduction of boronic acid functionality, boronate affinity materials exhibit several significant advantages, including broad-spectrum selectivity, reversible covalent binding, pH-controlled capture/release, fast association/desorption kinetics, and good compatibility with mass spectrometry. Because *cis*-diol-containing biomolecules, including nucleosides, saccharides, glycans, glycoproteins and so on, are the important targets in current research frontiers such as metabolomics, glycomics and proteomics, boronate affinity materials have gained rapid development and found increasing applications in the last decade. In this review, we critically survey recent advances of boronate affinity materials. We focus on fundamental considerations as well as important progresses and new boronate affinity materials reported in the last decade. We particularly discuss on the effects of the structure of boronate ligands and supporting materials on the properties of boronate affinity materials, such as binding pH, affinity, selectivity, binding capacity, tolerance for interference and so on. A variety of promising applications, including affinity separation, proteomics, metabolomics, disease diagnostics and aptamer selection, are introduced with main emphasis on how the boronate affinity materials can solve the issues in the applications and what merits the boronate affinity materials can provide.

## 1. Introduction

*Cis*-diol-containing biomolecules, such as nucleosides, saccharides, glycans and glycoproteins, are the important targets in current research frontiers such as metabolomics, glycomics and proteomics. Many *cis*-diol-containing biomolecules of research and clinical importance usually exist in very low abundance in biological systems meanwhile high-abundance interfering components co-exist. Therefore, the selective enrichment is usually a critical step for the analysis of *cis*-diol-containing biomolecules. As a unique means for the selective separation and enrichment of *cis*-diol-containing biomolecules, boronate affinity materials have gained increasing attentions in the last decade.<sup>1-3</sup>

The binding reaction between boric acid and *cis*-diols was discovered more than 170 years ago.<sup>4</sup> By the 1930s, the reaction of boric acid with *cis*-diols had been used to investigate the influence of various sugar alcohols and their anhydrides on the dissociation of boric acid.<sup>5</sup> In the 1940s, the interaction between

boric acid and *cis*-diols was employed as a tool for the analysis of carbohydrates.<sup>6</sup> In the 1950s, Foster<sup>7</sup> realized zone electrophoretic separation of carbohydrates by virtue of borate/*cis*-diols interactions, while Sugihara and co-workers<sup>8</sup> performed a comparative study on the binding abilities of boric and boronic acids toward different *cis*-diols. In the 1960s, a borate solution was added to the solvent system in paper chromatography for the separation of compounds containing orthophosphate and sugar phosphates.<sup>9</sup> However, boronic acid-functionalized materials had not appeared until Weith and co-workers<sup>10</sup> reported the first boronic acid-modified cellulose stationary phase for column chromatographic separation of standard mixtures of deoxyribo- and ribonucleosides in 1970. Within the next three decades, although a lot of boronate affinity materials had been developed,<sup>11-32</sup> they were mainly conventional chromatographic media, such as cellulose, polyacrylamide, agarose or Sepharose and sephacryl gels. The most important application of these boronate affinity materials was the selective



Daojin Li received his Bachelor degree from Shangqiu Normal University in 2004. After He received his Master degree from Lanzhou University in 2007, he joined Luoyang Normal University as a lecturer. In 2012, he entered Nanjing University to pursue Ph.D. study under the supervision of Prof. Zhen Liu. His research interests include optical spectroscopy, advanced functional materials and their applications in bioanalysis and bioseparation. He has published 27 peer-reviewed journal

papers.

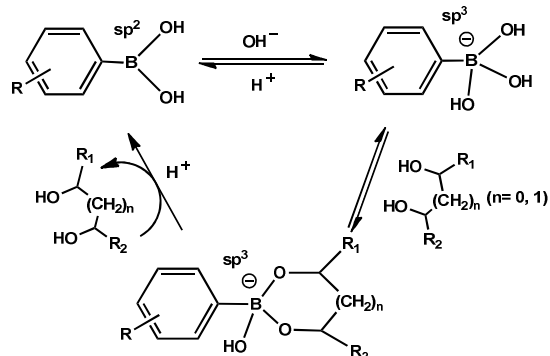


Yang Chen received his Bachelor degree from Anhui Normal University in 2011. He obtained his Master degree from Nanjing University under the supervision of Prof. Zhen Liu in 2014. He is currently a Ph. D. candidate in Dr. Zhen Liu's group at Nanjing University. His research interests include advanced affinity materials and their applications in molecular recognition and bioseparation. He has published 8 peer-reviewed journal

papers.

isolation of glycosylated hemoglobin for the clinic diagnosis of diabetic mellitus.<sup>16,17,21,22,25,28</sup> In the last decade, due to the rapid development of x-omics particularly proteomics, metabolomics and glycomics, boronate affinity materials have entered into a new age. A variety of new boronate affinity materials, such as macroporous monoliths,<sup>33-60</sup> mesoporous materials,<sup>61-63</sup> nanoparticles,<sup>64-88</sup> molecularly imprinted polymers,<sup>89-112</sup> and temperature-responsive materials,<sup>113-121</sup> have been developed rapidly for the separation of various *cis*-diol-containing compounds, including nucleosides, nucleotides, nucleic acids, catechols, carbohydrates and glycoproteins. Very importantly, some fundamental issues, such as binding pH, affinity and selectivity, have been well solved in this decade. With these efforts, boronate affinity materials have gained apparently improved binding properties and found increasing practical applications such as clinical diagnosis. To mimic the pH-controlled binding properties of boronate affinity materials, nanoconfining affinity materials<sup>122</sup> have been developed, in which the affinity ligands are other functionality groups rather than boronic acids.

The principle of molecular interactions of boronate affinity materials relies on the reversible covalent reaction between boronic acid ligands and *cis*-diol-containing compounds. Scheme 1 shows a general formula for the interaction between a boronic acid and a *cis*-diol-containing compound. When the surrounding pH is greater than the  $pK_a$  value of the boronic acid, the boronic acid presents as the form of a tetragonal boronate anion ( $sp^3$ ) and it can react with *cis*-diols and form five or six-membered cyclic esters. When the pH of the surrounding solution is switched to acidic, the boronic acid-*cis*-diol complex dissociates because under such a pH condition the boronic acid presents as a trigonal configuration ( $sp^2$ ) and the binding between the  $sp^2$  form of the boronic acid and *cis*-diol-containing compounds is usually very limited.



**Scheme 1** Schematic of the interaction between boronic acids and *cis*-diol-containing compounds.

Separation and molecular recognition by boronate affinity materials depend on their binding properties, especially binding pH, affinity and selectivity. The binding pH and affinity of boronate affinity materials are determined by the structure of the boronic acid, which can be roughly predicted by the  $pK_a$  value of boronic acid ligand. In general, the lower the  $pK_a$  value of a boronic acid ligand is the lower the binding pH and the higher the binding affinity it can provide. Besides, the structure of supporting materials also influences the binding pH and binding affinity of boronate affinity materials. Especially, spatial confinement of molecularly imprinted cavities and nanoscale pores can significantly lower binding pH and enhance binding affinity. Moreover, ligand structure and material structure can apparently affect the selectivity of boronate affinity materials. In

addition to boronate affinity interaction, several secondary interactions, mainly including hydrophobic, ionic and hydrogen bonding, can occur on boronate affinity materials. These interactions highly depend on the structure of the boronate ligand and supporting material used. By choosing appropriate boronate ligand and supporting material, secondary interactions can be suppressed.

The pH of frequently used biological samples, such as blood, tear, urine and saliva, ranges from 4.5 to 8.0. 3-aminophenylboronic acid (APBA) and 4-vinylphenylboronic acid (VPBA) are the most widely used boronate ligands, which have a  $pK_a$  value of 8.8 and 8.2, respectively. Therefore, conventional boronate affinity materials, in which the ligands predominantly determine the binding properties, cannot be directly applied to these biosamples. On the other hand, since the concentration of *cis*-diol-containing biomolecules of interests in biological samples is generally very low while high-abundance interfering species co-exist in the sample matrix, capture of target *cis*-diol-containing biomolecules by conventional boronate affinity materials, which are associated with low affinity and specificity, is rather difficult or impossible. Clearly, desired binding properties, especially low binding pH, high binding affinity and high binding specificity, are critical for real-world applications.

The synthesis and applications of boronic acid-containing polymers in biomedical areas, such as glucose sensors and drug delivery have been reviewed.<sup>123,124</sup> Advances in monolithic column-based boronate affinity chromatography (BAC) have been also reviewed.<sup>2</sup> However, a review focusing on the recent advances in boronate affinity materials for separation and molecular recognition is apparently lacking. In particular, fundamental issues encountered, such as how ligand structure and material structure affect the properties of boronate affinity materials, must be deeply analyzed and reviewed, which can further promote the development and applications of boronate affinity materials in future. In this review, we survey recent progresses of boronate affinity materials. We focus on fundamental considerations as well as important advances and new boronate affinity materials reported in the last decade. We particularly discuss on the effects of the structure of boronate ligands and supporting materials on the properties of boronate affinity materials, such as binding pH, affinity, selectivity, binding capacity, tolerance for interference and so on. A variety of promising applications, including affinity separation, proteomics, metabolomics, disease diagnostics and aptamer



Dr. Zhen Liu obtained his Ph.D. from Dalian Institute of Chemical Physics, Chinese Academy of Sciences in 1998. He was appointed as a full professor at Nanjing University in 2005. He was awarded the title "New Century Excellent Talents in Universities" by the Ministry of Education of China in 2008 and the National Science Fund for Distinguished Young Scholars in 2014. His current major research interest is to develop advanced functional materials and innovative approaches for molecular recognition, separation, bioanalysis and disease diagnosis. He has published 1 monograph, 5 book chapters and 110 peer-reviewed journal papers.

selection, are introduced with emphasis on the issues that boronate affinity materials can solve in the applications and the merits that boronate affinity materials can provide.

## 2. Structure and properties

### 2.1 Ligand structure and the properties

As discussed above, the binding properties of boronate affinity materials, especially binding pH, binding affinity, binding selectivity and binding capacity, are greatly determined by the structure of boronic acid ligands. In order to prepare boronate affinity materials with desired properties, numerous attempts have been made.<sup>2,26,37,41,45-49,52,57,73,75,85,125</sup> The ligands used so far can be classified into the following three categories.

#### 2.1.1. Single ligands

Single ligands mean that the boronate ligands employed function individually, among which there are no synergistic actions. This is usually true when the target compound contains only one pair of *cis*-diol group. This is also often the real situation when the target compounds contain multiple *cis*-diol groups but the density or location of boronate ligand is unfavourable for simultaneous multiple binding. In such a case, the structure of boronate ligand significantly affects the binding properties of boronate affinity materials particularly binding pH, binding affinity and binding selectivity.

Binding pH is a critical factor for boronate affinity. Usually a lowest binding pH is provided to indicate the lowest pH condition of the sample environment a boronate affinity material can work. Although the total number of commercially available boronic acids and derivatives is more than 1500, the lack of active moieties of commercially available boronic acids hampers their immobilization onto supporting materials. VPBA and APBA, which have active moieties, are two widely used boronic acid ligands for boronate affinity materials. However, because of their relatively high  $pK_a$  values, conventional boronate affinity materials usually require a basic pH for binding (usually the pH should be  $\geq$  the  $pK_a$  value of the boronic acid ligand). Since the pH of frequently used biosamples ranges from 4.5 to 8.0, the use of a basic pH gives rise to not only the inconvenience of pH adjustment, but also the risk of degradation of labile biomolecules. To reduce the binding pH, boronic acids with special structures that allow for binding *cis*-diol-containing compounds in a real sample pH environment are in great demand.

So far, four types of boronic acids can provide low binding pH: I) boronic acid ligands with electron-withdrawing groups, such as nitro, fluoro, sulfonyl and carbonyl on the phenyl ring;<sup>52,125-127</sup> II) Wulff-type boronic acids, which contain intramolecular tetracoordinated B-N or B-O bond;<sup>18,26,128</sup> III) improved Wulff-type boronic acids, which contain intramolecular tricoordinated B-O bond;<sup>129-131</sup> and IV) heterocyclic boronic acids.<sup>57,132,133</sup> Table 1 shows the structures of boronic acid ligands with low  $pK_a$  values that can be used to prepare boronate affinity materials with low binding pH.

For boronic acid ligands with electron-withdrawing groups, the presence of electron-withdrawing substituents in the aryl group increases the acidity and lowers the  $pK_a$  value. Representatives of this type of boronic acids include 4-(3-butenylsulfonyl) phenylboronic acid (BSPBA) and 2,4-difluoro-3-formyl-phenylboronic acid (DFFPBA). BSPBA, with sulfonyl group on para- position of phenyl ring, exhibited a  $pK_a$  of 7.0.<sup>125</sup>

A BSPBA-functionalized silica gel allowed for binding *cis*-diol-containing compounds at near neutral pH.<sup>125</sup> In addition, a poly (BSPBA-co-MBAA) monolithic column exhibited strong affinity for *cis*-diol-containing molecules at neutral pH.<sup>39</sup> DFFPBA exhibits a relatively low  $pK_a$  value (6.5).<sup>52</sup> DFFPBA-functionalized monolithic columns with varying spacer arms retained *cis*-diol-containing compounds under neutral and medium acidic pH conditions.<sup>52</sup>

**Table 1** The structures of boronic acids with low  $pK_a$  values.

Type	Structure	Name	$pK_a$	Ref.
Boronic acid with electron-withdrawing groups		4-(3-butenylsulfonyl) phenylboronic acid	7.0	[125]
		4-(N-allylsulfamoyl) phenylboronic acid	7.3	[125]
		(3-amino-4-nitrophenyl) boronic acid	7.5	[126]
		3-acrylamido phenylboronic acid	8.2	[47]
		4-(1,6-dioxo-2,5-diaza-7-oxamyl) phenylboronic acid	7.8	[127]
		3-(pent-4-ynamido) phenylboronic acid	8.2	[48]
		2,4-difluoro-3-formyl phenylboronic acid	6.5	[52]
Wulff type boronic acid		3-(dimethylaminomethyl) aniline-4-boronic acid	5.2	[18]
		2-(diethylamino)carbonyl-4-bromomethyl phenylboronic acid	—	—
Improved Wulff type boronic acid		3-carboxybenzoborazole	6.9	[46]
Heterocyclic boronic acids		3-pyridinylboronic acid	4.4	[132]
		2-aminopyrimidine-5-boronic acid	—	—
		3-thiopheneboronic acid	—	—

Wulff-type boronic acids that contain intramolecular tetracoordinated B-N bond can exhibit a  $pK_a$  value as low as 5.2.<sup>18</sup> With the presence of B-N bond, hybridization status of B atom changes from trigonal coplanar shape ( $sp^2$ ) to tetragonal boronate anion ( $sp^3$ ). The  $sp^3$  hybridization status keeps unchanged even under neutral or medium acidic conditions, which is favourable for boronate esterification with *cis*-diol-containing compounds. Although Wulff-type boronic acids have been employed in biological sensing,<sup>134,135</sup> commercially available Wulff-type boronic acids usually do not carry a reactive moiety for immobilization onto supporting materials. This limits the application of Wulff-type boronic acids in separation and molecular recognition. Liu and co-workers<sup>41</sup> synthesized a Wulff-type boronate with an amine group in the molecular structure, namely, 3-(dimethylaminomethyl) aniline-4-pinacol boronate (DMAMAPB). The presence of the electron-donating amino group may slightly increase the  $pK_a$  value. A DMAMAPB-functionalized monolithic column retained *cis*-diol-containing compounds at pH as low as 5.5. In addition, Scouten and co-workers<sup>26</sup> prepared another Wulff-type boronate affinity ligand,

namely, catechol [2-(diethylamino) carbonyl-4-bromomethyl] phenylboronate (DECBP), which contains intramolecular tetracoordinated B-O bond between a carbonyl oxygen and a boron atom. This type of coordination makes the boron atom tetrahedral, which is favourable for the reaction of boronate with *cis*-diol-containing compounds. DECBP-functionalized cellulose beads allowed for the capture of glycoproteins such as horseradish peroxidase (HRP) at pH 7.0.

Benzoboroxoles, which are called improved Wulff-type boronic acids, contain intramolecular tricoordinated B-O bond rather than the classical intramolecular tetracoordinated B-N or B-O bond in the molecular structure. Due to their unique structure, they showed excellent water solubility and improved sugar binding capability, even superior to Wulff-type boronic acid in neutral water. Liu and co-workers<sup>46</sup> synthesized 3-carboxybenzoboroxole and immobilized it onto a monolithic column. Although the  $pK_a$  value is not significantly low (6.9), the 3-carboxybenzoboroxole-immobilized monolithic column could bind with *cis*-diol-containing biomolecules such as nucleosides even at pH 5.0.

In comparison to phenylboronic acid, heterocyclic boronic acids can exhibit apparently lower binding pH due to the presence of a hetero atom (N, O, or S) in the ring. Pyridinylboronic acids, which contain a nitrogen atom in the heterocyclic ring, exhibit very low  $pK_a$  values due to the presence of a zwitterion in weak acidic solutions. For example, 3-pyridinylboronic acid has a  $pK_a$  value of 4.4.<sup>132,133</sup> Recently, a 3-pyridinylboronic acid-functionalized monolithic column has been developed.<sup>57</sup> It permitted the selective capture of *cis*-diol-containing compounds at pH as low as 4.5, which was the lowest among all the reported boronate affinity materials. However, the reactivity of the N atom is very weak so that the modification of 3-pyridinylboronic acid onto a chloropropyl-functionalized monolithic column took 4 days at 75°C.<sup>57</sup> Owing to the presence of two N atoms in its molecular structure, the acidity of pyrimidine-5-boronic acid is much higher than that of pyridinylboronic acid, which results in extremely high affinity at weak acidic pH.<sup>136</sup> However, it is rather hard to immobilize pyrimidine-5-boronic acid onto supporting materials because of the absence of a reactive moiety. 2-Aminopyrimidine-5-boronic acid, which is available from Sigma-Aldrich, contains a reactive amino moiety and therefore can be easily attached to a supporting material. However, a 2-aminopyrimidine-5-boronic acid-functionalized monolithic column could capture *cis*-diol compounds only when the pH was  $\geq 5.0$  (unpublished data). This can be explained by the fact that the amino moiety is an electron-donating group so that its presence might have offset the electron-withdrawing effect of the N atoms on the hetero ring.

As discussed above, the binding pH of boronate affinity materials is usually related to the  $pK_a$  value of the boronic acid. However, some other factors can also make a big difference. 3-acrylamidophenylboronic acid (AAPBA) has relatively high  $pK_a$  value (8.2). However, beyond normal expectation, two AAPBA-silica hybrid monolithic columns exhibited substantial *cis*-diol-binding capability at pH as low as 6.5 or 7.0.<sup>47,49</sup> A possible explanation is that the presence of an acrylamino group in the AAPBA molecule makes the geometry of the B atom turn into a  $sp^3$  configuration at a slightly acidic or neutral pH conditions. Similarly, both 3-(pent-4-ynamido)phenylboronic acid-silica hybrid monolithic column<sup>48</sup> and 3-(pent-4-ynamido)phenylboronic acid-functionalized  $Fe_3O_4$  hybrid composites<sup>84</sup> permitted the selective capture of glycoproteins

under physiological conditions. On the other hand, structurally special analytes<sup>137</sup> may also lead to the deviation from normal pattern. Sialic acid, as an example, exhibits anomalously high binding strength with common boronic acids at pH  $\ll pK_a$  due to the presence of B-N coordination between sialic acid and boronic acid.<sup>138</sup> Such an exception provides a molecular basis for the selective recognition of sialic acid against other saccharides using conventional boronic acid ligands.<sup>50</sup>

In general, the lower the binding pH value of a boronic acid is, the higher the binding strength it can provide. Therefore, boronic acids mentioned above obey similar effects of structures on the binding strength.

In addition to the above mentioned binding pH and binding affinity, selectivity is also a key property of boronate affinity materials, which greatly affects the performance of boronate affinity materials in the separation and enrichment of *cis*-diol-containing biomolecules. It is often a challenging task to selectively separate target molecules by means of boronate affinity, especially macromolecules. To realize boronate affinity-controlled separations, it is indispensable to establish a sound understanding of all interactions that a boronate affinity material may involve. Such a fundamental aspect has been systematically investigated in previous reports.<sup>2,139</sup> It was observed that in addition to boronate affinity interaction, several secondary interactions, mainly including hydrophobic interaction, ionic interaction and hydrogen bonding, can occur on boronate affinity materials. In general, higher boronate affinity favours selectivity. Apparently, boronic acid ligands with lower binding pH or higher binding affinity can lead to higher selectivity toward *cis*-diol-containing compounds. Meanwhile, the secondary interactions can also greatly affect the selectivity of boronate affinity materials.

Hydrophobic interaction is one main secondary interaction that influences the selectivity of boronate affinity. Boronic acid ligands used in affinity materials are usually aromatic boronic acids and thereby can give rise to hydrophobic interaction and aromatic  $\pi$ - $\pi$  interaction, which can cause nonspecific adsorption of analytes such as proteins. Fortunately, hydrophobic interaction can be reduced or eliminated by using hydrophilic boronate ligands. For example, a poly (VPBA-co-ethylene glycol dimethacrylate (EDMA)) monolith exhibited significant hydrophobicity,<sup>35</sup> which failed to capture glycoproteins selectively when no organic solvent was added to the binding buffer. After replacing the relatively hydrophobic boronic acid VPBA with relatively hydrophilic one, AAPBA,<sup>34,40</sup> the resultant poly (AAPBA-co-EDMA) monolith exhibited good selectivity toward glycoproteins, though the cross linker, EDMA, is not so hydrophilic. In another example, a VPBA-silica hybrid affinity monolith<sup>43</sup> could exhibit selective capture of *cis*-diol-containing compounds only if organic solvent such as acetonitrile was added to the binding buffer. After substituting VPBA with AAPBA, an AAPBA-silica hybrid affinity monolith<sup>47</sup> exhibited excellent selectivity toward *cis*-diol-containing compounds even with the absence of organic solvent in the binding buffer.

Ionic interaction is another major secondary interaction that influences the selectivity of boronate affinity materials. For a regular boronic acid ligand, the boron atom must be tetrahedral  $sp^3$  orbital hybridization status for eventual binding with *cis*-diol-containing compounds, at which the boron is negatively charged. Therefore, ionic interaction occurs for charged *cis*-diol-containing compounds. A solution to this issue can be the employment of Wulff-type boronic acid with intramolecular tetracoordinated B-N or B-O coordination due to their zero or limited apparent charge. For strongly negatively charged *cis*-diol-containing compounds, such as ribonucleotides, a solution to this issue is to



introduce pyridinium.<sup>57</sup>

Hydrogen bonding is an inevitable secondary interaction, because boronic acids always carry hydroxyl group(s). The effect of hydrogen bonding is usually negligible; however, in some situations, hydrogen bonding can be a major driving force for a secondary separation on a boronate affinity material. Recent publications<sup>39,47</sup> reported that highly hydrophilic boronate affinity columns exhibit apparent secondary separation capability toward *cis*-diol-containing compounds, which was attributed to hydrogen bonding interaction.

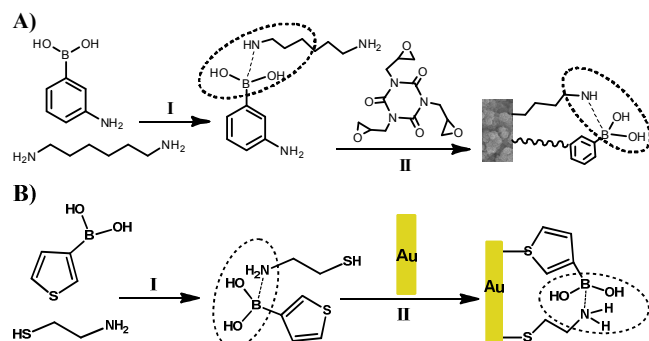


**Fig. 1** A) (I) B-N coordination and (II) ring-opening polymerization with synergistic co-monomers; Adapted from ref. 37 with permission from John Wiley and Sons. B) (I) B-N coordination and (II) self-assembly on the gold surface with synergistic co-monomers. Adapted from ref. 73 with permission from The Royal Society of Chemistry.

### 2.1.2. Molecular teams

For type I-III mentioned above, a boronic acid monomer with low binding pH, if not commercially available, must be synthesized and purified first through multistep reaction routes. For instance, the synthesis of a reactive group containing Wulff-type boronic acids, or improved Wulff-type boronic acids usually requires multiple steps (a four-step, three-step or two-step reaction route is needed to synthesize DMAMAPB, DECBP, or 3-carboxybenzoboroxole, respectively), which to some extent limits the application of these types of boronic acids in boronate affinity separation and recognition. Although a big variety of heterocyclic boronic acids (type IV) are commercially available, they are difficult to be modified onto supporting materials. These problems had driven Liu and co-workers to make much effort to obtain a high-affinity boronic acid ligand without tedious synthesis and purification. They proposed a new strategy called teamed boronate affinity (TBA).<sup>37,73</sup> The central concept of TBA is different from conventional boronate affinity, which relies on a single boronic acid alone. TBA turns on a “molecular team” that comprises a boronic acid (e.g., APBA or thiophene-3-boronic acid) and a neighbouring amine (e.g., 1, 6-hexamethylenediamine (HMDA) or 2-mercaptoethylamine (MPA)). By virtue of B-N coordination between the boronic acid and the amine, the two compounds can form a complex or a molecular team (Fig. 1). Through an appropriate reaction such as ring-opening polymerization<sup>37</sup> or molecular self-assembly,<sup>73</sup> the molecular team can be fixed onto a supporting material, and the resulting TBA material can function as a single Wulff-type boronic acid ligand to enable the capture of *cis*-diol-containing compounds under neutral conditions. When the surrounding pH is made more acidic, the amine group is protonated, and the B-N coordination is disrupted, which results in the release of the *cis*-diol-containing compounds from the TBA materials. Using the molecular team of *N*-( $\beta$ -aminoethyl)- $\gamma$ -aminopropyltriethoxysilane (AEAPTES) and

the VPBA as an affinity ligand, Zhou and co-workers<sup>54</sup> further prepared an organic-inorganic hybrid boronate affinity monolithic column through the sol-gel process and free radical polymerization. The resulting monolith could bind with *cis*-diol-containing compounds at neutral pH. As mentioned in 2.1.1, binding pH is inversely related to binding affinity. The molecular team-functionalized materials can exhibit higher binding strength than common boronic acid-functionalized materials. Accordingly, the higher binding affinity can also lead to higher selectivity. In addition, for charged *cis*-diol-containing compounds, B-N coordinated molecular team can reduce or eliminate ionic interaction owing to its zero or limited apparent charge, thus improving the selectivity. Obviously, the molecular team-functionalized materials provide significant advantages, such as simple procedure, low binding pH, high affinity and high selectivity. However, the applicable pH range of TBA is not so wide as compared with a Wulff-type boronic acid.

### 2.1.3. Dendrimeric boronic acids

The binding strength of single boronic acids or molecular teams toward *cis*-diol-containing biomolecules is relatively weak, with dissociation constants ( $K_d$ ) between boronic acids and sugars or glycoproteins ranging from  $10^{-1}$  to  $10^{-3}$  M.<sup>136,137</sup> Therefore, an effective solution to provide significantly high affinity is very important. Dendrimeric boronic acids were developed to respond such a demand, which was inspired by multiple binding in biomolecular interactions. Biomolecules such as antibodies can strongly bind with their target molecules, because of their avidity, through synergistic multiple binding rather than the affinity of a single binding. In fact, simultaneous multiple binding has proved to be an effective strategy for enhancing the binding strength.<sup>140,141</sup> Due to their multivalent binding sites, dendrimers,<sup>142,143</sup> which are highly branched and monodisperse macromolecules, have been useful scaffolds. Highly branched dendrimers have been used to amplify the number of boronic acid moieties. Using poly(amidoamine) (PAMAM) dendrimeric 4-formylphenylboronic acid (FPBA) as the affinity ligand, a type of boronate avidity magnetic nanoparticles (MNPs) exhibited significantly enhanced binding strength of  $10^{-5}$  to  $10^{-6}$  M toward glycoproteins due to the presence of multivalent synergistic binding, which is 3-4 orders of magnitude higher than the affinity of single boronic acid binding.<sup>80</sup> Fig. 2 depicts synergistic multiple binding between a glycoprotein and PAMAM-amplified boronate avidity MNPs. Because the high density of the amino groups on the PAMAM supplied a large number of binding sites for boronate groups, the binding capacity of the nanoparticles (NPs) for adenosine was improved by 3- to 4-fold as compared with that of analogous materials without PAMAM. However, the highly branched PAMAM dendrimers are associated with apparent disadvantages, such as high cost and strong rigidity. The rigid structure is unfavourable for effective enrichment and quick equilibration.

Branched polyethyleneimine (PEI) contains flexible chains, which can reduce the steric hindrance when it is used as a spacer arm. Besides, it is hydrophilic and inexpensive. In this sense, PEI can be a more ideal scaffold to prepare dendrimeric boronic acid. Using a PEI dendrimeric boronic acid as the affinity ligand, Xu and co-workers<sup>78</sup> prepared a PEI-assisted hybrid MNPs ( $\text{Fe}_3\text{O}_4@SiO_2@PEI-FPBA$ ). Due to the flexible feature and a large number of binding sites of PEI, the NPs exhibited significantly improved adsorption capacity ( $1.34 \pm 0.024$  mg/g), which was 6- to 7-fold higher than that of similar materials without the amplification effect of PEI or PAMAM. The  $\text{Fe}_3\text{O}_4@SiO_2@PEI-FPBA$  provided 2-3 times higher adsorption capacity as compared with the PAMAM-amplified boronate

avidity MNPs. Moreover, the flexible chains of PEI were favourable for quick equilibration (< 2 min). In order to further develop boronate avidity materials with higher binding strength, Liu and co-workers<sup>60</sup> prepared a PEI dendrimeric boronic acid-functionalized monolithic column (PDMC) with high avidity for the selective enrichment of trace glycoproteins. Monolithic column was selected as base material because it is more challenging to prepare boronate avidity monolithic columns as compared with MNPs. DFFPBA was used as an affinity ligand because it exhibited ultrahigh affinity toward *cis*-diol-containing compounds at neutral or medium acidic pH condition. The PDMC exhibited  $K_d$  values of  $10^{-6}$ - $10^{-7}$  M for glycoproteins, which are lower by 1-2 orders of magnitude than that of a monolithic capillary prepared with the same approach using ethylenediamine (EDA) as a substitute of PEI (EDMC). The binding strength of PDMC toward glycoproteins is comparable with the low end of binding strength of antibodies ( $K_d$  value usually  $10^{-7}$ - $10^{-9}$  M), which was the highest among already reported boronic acid-functionalized materials that can be used for comprehensive extraction of glycoproteins against nonglycoproteins. The  $K_d$  value of PDMC is lower than that of the PAMAM-amplified boronate avidity MNPs by 1 order of magnitude. This was attributed to the ultrahigh affinity of DFFPBA and flexibility of PEI as well as the confinement effect of nanopores of the monolithic capillary. Moreover, the PDMC column exhibited lowered binding pH ( $\geq 6.5$ ) toward glycoproteins due to its higher binding strength, which was 1 pH unit lower than that of EDMC. These features greatly favoured the selective enrichment of trace glycoproteins from real samples. In comparison, capture of *cis*-diol-containing biomolecules such as glycoproteins of very low concentration by conventional boronate affinity materials is rather difficult or even impossible. However, it is worthy to notice that unfavourable electrostatic interactions may occur on this type of boronate avidity materials due to the presence of plentiful amino moieties particularly secondary and tertiary amino groups, which will influence the selectivity toward charged *cis*-diol compounds.

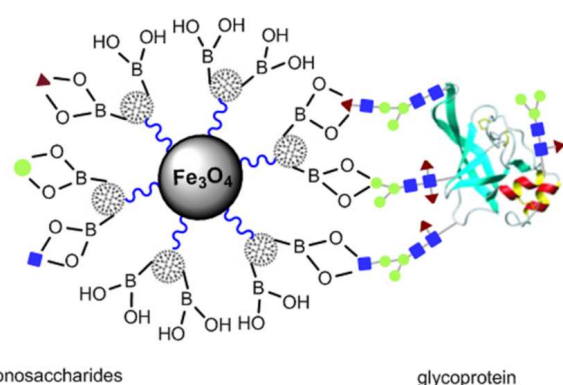


**Fig. 2** Principle of enhancing the binding strength of boronic acid-functionalized MNPs toward glycoproteins via dendrimer-assisted multivalent synergistic binding. Reproduced from ref. 80 with permission from The Royal Society of Chemistry.

It must be pointed out that the synergistic effect of dendrimeric boronic acids is only applicable to compounds containing multiple *cis*-diol groups such as glycoproteins. For single *cis*-diol group-containing compounds such as adenosine, the employment of dendrimeric boronic acids fails to provide improved binding strength. For instance, the PDMC and EDMC columns exhibited comparable binding constants toward adenosine, with  $K_d$  values of  $(4.62 \pm 0.58)$  and  $(7.18 \pm 0.88)$

$\times 10^{-4}$  M, respectively.<sup>60</sup> However, the use of dendrimeric boronic acids can provide improved binding capacity toward single *cis*-diol group-containing compounds. The binding capacity of the PDMC and EDMC columns for adenosine was  $102.10 \pm 8.47$  and  $26.53 \pm 2.20$   $\mu\text{mol/g}$ , respectively. As a comparison, the employment of dendrimeric boronic acids usually fails to enhance the binding capacity for glycoproteins. The PDMC and EDMC columns exhibited comparable binding capacity for HRP, being  $0.32 \pm 0.03$  and  $0.35 \pm 0.01$   $\mu\text{mol/g}$ , respectively.

## 2.2. Material structure and the properties

In addition to boronic acid ligands, material structure also has significant effects on the properties of boronate affinity materials, such as binding pH, affinity, selectivity, binding capacity, tolerance for interference, and so on. A few new material structure formats have been developed for boronate affinity separation and recognition of *cis*-diol-containing compounds, including macroporous monoliths, mesoporous materials, nanoparticles, molecularly imprinted polymers, and temperature-responsive materials. Besides, nanoconfining affinity materials with boronate affinity-like binding behaviours have been developed recently.

### 2.2.1. Macroporous monoliths

Macroporous monoliths or monolithic columns, pioneered by Hjerten,<sup>144</sup> Svec<sup>145</sup> and Tanaka,<sup>146</sup> are defined as “continuous stationary phases that form as a homogeneous column in a single piece”. As compared with conventional chromatographic columns, monolithic columns can provide several significant advantages such as ease of preparation, low cost, low back pressure, fast convective mass transfer and ease of miniaturization in channels and capillaries. Especially, monolithic capillaries-based high-performance liquid chromatography (HPLC) has the attractive properties of improved chromatographic resolution, higher efficiency, lower sample consumption, more convenient online coupling to mass spectrometry (MS) and improved mass-detection sensitivity, as compared with classical columns-based HPLC.

Although monolithic columns had appeared since 1990s, boronate affinity monolithic column was first reported in 2006.<sup>33</sup> Since then, boronate affinity monolithic columns have been rapidly developed because of the merits of both boronate affinity and monolithic columns.<sup>33-60</sup> According to the nature of monolithic materials structure, boronate affinity monolithic columns appeared so far can be classified into the following two categories: 1) boronate affinity organic polymer monolithic columns, and 2) boronate affinity organic-inorganic hybrid monolithic columns.

#### 2.2.1.1. Boronate affinity organic polymer monolithic columns

Organic polymer monolithic columns have good stability toward pH changes and great flexibility to tune the surface chemistry as well as easy preparation. Thus, boronate affinity organic polymer monolithic columns have been widely developed.<sup>33-42,44-46,50,52,53,56,59,60</sup> For example, a VPBA or 4-hydroxyphenylboronic acid-functionalized monolithic column using EDMA as crosslinker exhibited highly selective separation of *cis*-diol-containing small molecules.<sup>33,35</sup> However, the monolithic columns failed to selectively separate glycoproteins due to apparent hydrophobicity, which was mainly attributed to hydrophobic structure of the crosslinker. After replacing EDMA with a hydrophilic cross-linker, *N,N'*-methylenebisacrylamide (MBAA), reversed-phase retention on the poly (VPBA-co-MBAA) monolith was reduced by 70% and the monolithic capillary exhibited good selectivity toward glycoproteins.<sup>36</sup> The

combination of a hydrophilic cross-linker with a hydrophilic affinity ligand produced a more hydrophilic monolithic column. For example, a poly (BSPBA-co-MBAA) monolithic column exhibited a highly hydrophilic nature and thereby showed excellent selectivity toward *cis*-diol-containing compounds particularly glycoproteins.<sup>39</sup>

In addition to the matrices of the materials, the nanopores size and shape of macroporous monoliths also have a significant influence on the properties of boronate affinity materials. It is well known that nanometer scale mesopores can provide unique size selectivity, which allows for free passage of small molecules inside but hampers the entrance of macromolecules. Such size exclusion effects have been employed as the core selectivity in many functionalized materials, such as restricted access materials<sup>147</sup> and mesoporous silica particles,<sup>148,149</sup> for the selective extraction of small molecules. Liu and co-workers<sup>45</sup> developed a protein A-like porous functionalized material, called restricted access boronate affinity porous monolith for the specific capture of immunoglobulin G (IgG). 4-Mercaptophenylboronic acid (MPBA) and *N,N'*-bis(2-aminoethyl)oxamide (BAEO) were chosen as team members to form a molecular team. MPBA was selected because of the absence of B-N coordination between MPBA molecules. BAEO was selected because of its hydrophilic nature. Ring-opening polymerization was used to make monolith because it can produce the highly ordered 3D skeletal polymer monoliths,<sup>146</sup> which successfully overcome to some extent the inherent disadvantages such as heterogeneous (irregular) microstructures caused by free radical polymerization. The specificity of the resulting restricted access boronate affinity porous monolith toward antibodies relies on combination of the chemical affinity and selectivity of boronic acids with the size selectivity of nanopores of macroporous monoliths. In addition to macropores of 1.44  $\mu\text{m}$ , the monolith possessed mesopores of 3.88 nm, which hampers the entrance of macromolecules such as glycoproteins. Uniquely, the TBA ligands well-located within mesopores, allowing for holding the whole antibody molecule outside of the mesopores via specifically binding with the Fc-glycan of IgG as depicted in Fig. 3. Other glycoproteins, despite containing glycan(s), are not captured due to the glycan cannot reach the boronic acid ligand within the mesopores. This restricted access boronate affinity porous monolith exhibited protein A-like specificity toward IgG. However, as compared with protein A, the biomimetic monolith exhibited significant advantages, including low cost, high stability and fast elution kinetics.

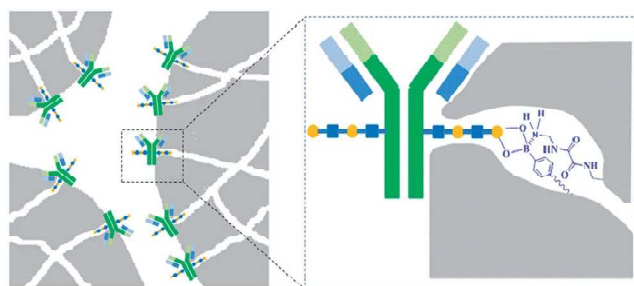


**Fig. 3** Schematic for specific recognition of IgG by the restricted access boronate affinity porous monolith. Reproduced from ref. 45 with permission from The Royal Society of Chemistry.

The density of the accessible boronic acid ligand on the material surface is also an important factor that affects boronate affinity interaction for compounds containing multiple *cis*-diol groups such as glycoproteins. A higher density always favours boronate affinity. However, it is difficult to predict the density of

accessible affinity ligand under synthesis route and procedure of boronate affinity materials. A reasonable solution is to immobilize an appropriate boronic acid ligand onto supporting materials with high specific surface area and high density of accessible reactive functional groups. To this end, Zhang and co-workers<sup>59</sup> developed a structurally unique boronate affinity monolithic capillary by immobilizing MPBA and MPA onto a gold nanoparticle-modified base monolith. The gold matrix provided advantages of good hydrophilicity and enhanced surface area, which could enhance boronate affinity, and thus improved the enrichment selectivity and efficiency for glycoproteins. Besides, the attachment of MPBA and MPA provided intramolecular B-N coordination, which could further enhance the affinity and specificity toward glycoproteins. Although the modification with gold NPs can greatly improve the hydrophilicity and binding capacity, a remarkable loss in permeability of the column is inevitable.

### 2.2.1.2. Boronate affinity organic-inorganic hybrid monolithic columns

Organic monolithic columns are associated with several disadvantages, including swelling in organic solvents, deficiency in mechanical stability, low surface area and low permeability. As a comparison, inorganic monolithic columns exhibit good solvent resistance to swelling, high mechanical stability, large surface area and high permeability. Nevertheless, the preparation process of inorganic monolithic columns is complicated and the pH stability is a little bit poor. Due to the virtues inherited from both sides of organic and inorganic monolithic columns, boronate-based organic-inorganic hybrid monolithic columns have gained rapid development in the recent years.<sup>43,47-49,51,54,55,57,58</sup> Lin and co-workers<sup>43</sup> first reported a phenylboronic acid-silica hybrid monolithic column using a one-pot approach. The scheme for the synthesis of VPBA-silica hybrid affinity monolith and its recognition mechanism toward glycoproteins is illustrated in Fig. 4. The preparation procedure included two major reactions: (1) polycondensation of the hydrolyzed tetramethyloxysilane (TMOS) and trialkoxysilanes with vinyl groups (3-methacryloxypropyltrimethoxysilane ( $\gamma$ -MAPS)) at a relatively low temperature (40  $^{\circ}\text{C}$ ), and (2) the radical copolymerization of precondensated siloxanes and the VPBA at a relatively high temperature (75  $^{\circ}\text{C}$ ). By optimizing experimental parameters such as the ratio of TMOS/ $\gamma$ -MAPS, the amount of VPBA, the choice of porogen and polymerization temperature, the resulting boronate affinity hybrid monolith exhibited an average pore diameter of 15.2 nm. The monolithic column with this type of porous structure permitted the entrance of macromolecules. Thus, the prepared monolith allowed for selective capture of glycoproteins and *cis*-diol-containing small biomolecules at basic pH conditions.

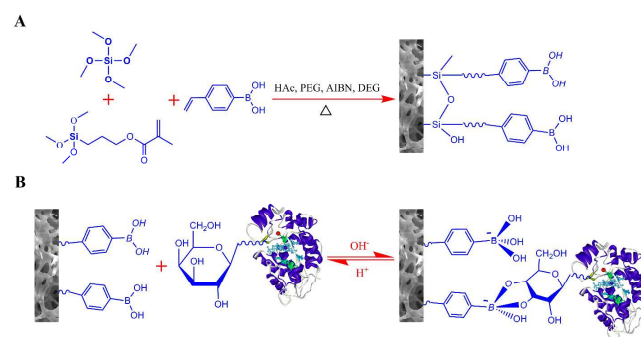


**Fig. 4** Schematic representation of (A) one-pot synthesis of VPBA-silica hybrid monolithic column and (B) its recognition



mechanism toward glycoproteins. PEG: poly (ethylene glycol); DEG: diethylene glycol; AIBN: 2,2-azobisisobutyronitrile. Reproduced from ref. 43 with permission from The Royal Society of Chemistry.

However, the above mentioned hybrid monolithic column exhibited a low surface area (35.2 m<sup>2</sup>/g) and low binding affinity. In order to address the issue, Liu and co-workers<sup>47</sup> developed an AAPBA-silica hybrid monolithic column by “one-pot” synthetic approach. AAPBA was used as the boronate affinity ligand owing to its relatively low pK<sub>a</sub> value (8.2) and more hydrophilic nature as compared to VPBA. The resulting AAPBA-silica hybrid monolith exhibited a large specific surface area (182.5 m<sup>2</sup>/g), which is higher than that of the VPBA-silica hybrid monolith. The monolith provided an extremely high binding capacity, 49.5 μmol/mL at pH 8.5, which is the highest among all the boronate affinity monolithic columns reported in the literature so far. The monolith allowed for selective capture of small *cis*-diol-containing biomolecules, but failed to capture *cis*-diol-containing biomacromolecule such as glycoproteins. A possible reason was the small average pore size (2.6 nm), which excluded macromolecules. This feature greatly favours the selective enrichment of small *cis*-diol-containing biomolecules from complex samples such as serum.

Although the VPBA-silica hybrid monolith could retain glycoproteins, its binding capacity for glycoproteins is low. The binding capacity for ovalbumin (OVA) at pH 8.0 was only 0.22 mg/g.<sup>43</sup> In order to improve the binding capacity for glycoproteins, a novel and efficient method for the preparation of a boronate affinity hybrid monolithic column was developed using Cu (I)-catalyzed 1,3-dipolar azide-alkyne cycloaddition (CuAAC) click reaction.<sup>48</sup> Click chemistry is an appealing synthetic approach proposed by Sharpless and co-workers.<sup>150</sup> It is a set of powerful, highly reliable, and selective reactions for the rapid synthesis of useful new compounds. Especially, CuAAC reaction was usually used as an efficient and simple strategy to generate various functional materials<sup>151</sup> owing to its unique advantages such as mild reaction conditions, high compatibility with a variety of functional groups, high yields and lack of side reactions. To prepare a boronate affinity hybrid monolith, an azide-functionalized hybrid monolith was first synthesized via a single-step procedure, and then the alkyne-boronate ligands were covalently immobilized onto the azide-functionalized hybrid monolith via CuAAC reaction. Although the total surface area of the resulting hybrid monolith (17.69 m<sup>2</sup>/g) was lower than that of the VPBA-silica hybrid monolith, it exhibited 24-fold higher binding capacity for OVA (5.35 mg/g) at pH 8.0 than the VPBA-silica hybrid monolith did. This reason is thought to be that the unique advantages of CuAAC reaction led to a higher density of accessible boronic acid functional groups on the monolith than that on traditional monoliths.

In addition to SiO<sub>2</sub> hybrid boronate affinity monolithic column, unique boronate-functionalized SiO<sub>2</sub>/TiO<sub>2</sub> hybrid monolithic column was synthesized<sup>58</sup> by using tetrabutyl orthotitanate (TBOT), tetraethoxysilane (TEOS), AEAPTES, and γ-MAPS as the co-precursors and cetyltrimethylammonium bromide (CTAB) as the template, beneficial to the homogeneity and permeability. The scheme for the synthesis of this monolithic column and its recognition mechanism to the *cis*-diol-containing analytes are illustrated in Fig. 5. The VPBA-functionalized hybrid monolith exhibited strong affinity and excellent selectivity toward glycoproteins including antibodies under the neutral/weakly acidic conditions (as low as pH 6.0). This lower binding pH was attributed to the formation of Ti-O-B bond. The strong electron-withdrawing effects of titanium (IV) ions could cause a decreased

electron density on the boron atom, making the boronic acid more acidic and thus greatly lowering the pK<sub>a</sub> value of the boronic acid. However, experimental evidences for the formation of Ti-O-B bond and its dependence on pH condition were not provided.

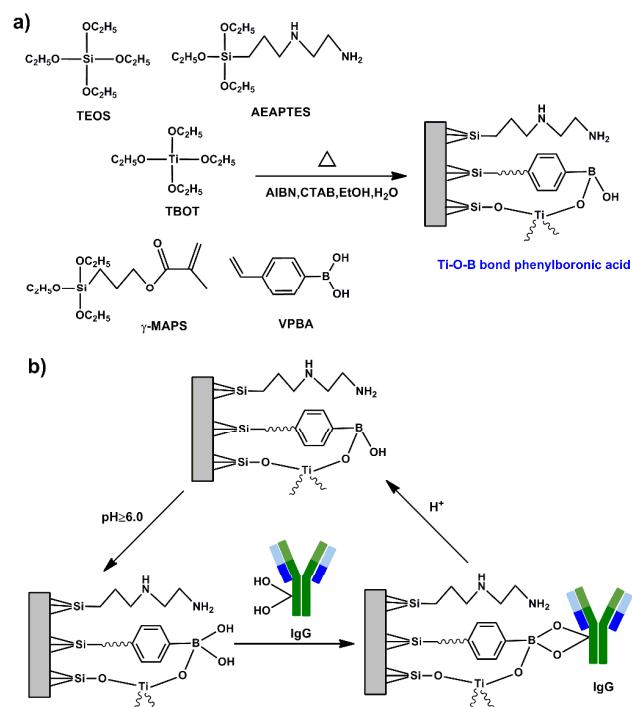


**Fig. 5** a) One-pot synthesis of the silica/titania hybrid boronate affinity monolithic column and b) reversible capture/release of IgG. Adapted from ref. 58 with permission from The Royal Society of Chemistry.

Besides, another monolithic borated titania was prepared through a simple non-aqueous sol-gel route,<sup>51</sup> which possessed a typical bimodal porosity with the rutile crystal form. The prepared borated titania was able to well capture *cis*-diol-containing molecules under neutral pH conditions and still retained obvious affinity toward glycoproteins even at pH 3.7, which avoids the need of a boronic acid ligand with low pK<sub>a</sub>. Unfortunately, the authors did not explain why the binding pH could be so low. This type of inorganic boronate affinity materials could be a new option for the separation and enrichment of the *cis*-diol-containing biomolecules at neutral pH conditions. However, no spacer arm seems to be an apparent disadvantage.

## 2.2.2. Mesoporous materials

Mesoporous materials possess a regularly ordered pore arrangement, high surface area, and very narrow pore size distribution. The first mesoporous materials known as MCM series were developed by scientists at the Mobil Oil Company.<sup>152</sup> Since this pioneering work, numerous synthetic strategies have been developed, providing a wide range of mesoporous materials (SBA,<sup>153</sup> FDU,<sup>154</sup> etc). The prominent features of mesoporous materials such as high surface area and narrow distribution of regular pore size, were well believed to lead to considerable advantages in analytical chemistry, especially separation and sample pretreatment. Among all kinds of mesoporous materials, mesoporous silica, with its ease in preparation and a large amount of surface silanol groups that can be easily modified with other functionalities, can be a greatly promising material for separation. The combination of boronate affinity with mesoporous silica

started from 2009, when Lu and co-workers reported a boronic acid-functionalized mesoporous silica for the enrichment of glycopeptides.<sup>61</sup> To satisfy different application purposes in separation, mesoporous silica with well controlled structures are highly desirable. According to Lu and co-workers, larger specific surface area and fast absorption/desorption kinetics are the key requirements of highly specific enrichment. In order to meet these requirements, they introduced the mesoporous silica FDU-12 as the matrix, which had three-dimensional pore system with large pore cavity and entrance size. A boronic acid-functionalized FDU-12 was synthesized through the post-graft method. The unique structure of FDU-12 greatly benefited its application in enrichment of glycopeptides. The loading and desorption time was shortened to only 15 min, much shorter than those of silica or magnetic beads (1 h). This fast mass transportation process was attributed to the high surface area and large entrance pore sizes of FDU-12. Moreover, the limit of detection (LOD) of this method was 435 amol/ $\mu$ L, nearly reduced by 2 orders of magnitude as compared with those of conventional methods. The recovery of glycopeptides was up to 83.5%. This good performance was attributed to the dramatically improved mass spectrometric (MS) detectability, which benefited from the elimination of the suppression effect of non-glycosylated peptides through the selective enrichment by boronic acid-functionalized FDU-12. However, the large entrance pore sizes of FDU-12 may lead to the relatively low surface area and thus decrease the binding capacity.

Another most significant feature of mesoporous materials is molecular sieve effect. Lu and co-workers<sup>62</sup> reported a boronic acid functionalized MCM-41 for the enrichment of endogenous glycopeptides. The small pore entrance size along with uniform mesoporous enabled exclusion of proteins with molecular weight (MW) larger than 20 kDa. This greatly benefited applications to complex samples. In addition, the high surface area guaranteed a high capacity for glycopeptides (40 mg/g). High selectivity (molar ratio of glycopeptides/non-glycopeptides is 1:100) and low LOD (fmol-level) were also two important merits benefited from the mesoporous structure.

### 2.2.3. Nanoparticles

NPs, with its relatively simpler synthetic procedure as compared with mesoporous materials, have attracted great attention from analytical chemists.<sup>155,156</sup> The abundant variability of chemical properties of NPs further extends the applicable range in separation science. A large variety of NPs have been successfully prepared for separation and molecular recognition in the past decade. The NPs reported so far could be roughly categorized into the following classes, including silica, organic polymers, lipids, metal oxides, and noble metal.<sup>157</sup> Due to the merits of the combination of both boronic acid and NPs, boronate functionalized NPs have become a hotspot for the highly efficient separation and molecular recognition of *cis*-diol-containing biomolecules in complex samples in recent decade.<sup>64-88</sup> Among these NPs, MNPs and magnetic composite are most widely used because of their good biocompatibility, superparamagnetic property, low toxicity, low cost and easy preparation.<sup>158,159</sup> Magnetic separation is a particularly effective technique for the separation of complicated samples due to its fast recovery, less disturbance and high efficiency.

Boronic acid-functionalized  $\text{Fe}_3\text{O}_4$  MNPs have been widely used for the separation and enrichment of *cis*-diol-containing biomolecules.<sup>64,75,80,83</sup> Deng and co-workers<sup>64</sup> synthesized amino-functionalized  $\text{Fe}_3\text{O}_4$  MNPs via a one-pot method and then APBA was modified onto the surface through hexanedioyl chloride bridge. The resulting  $\text{Fe}_3\text{O}_4$  MNPs were successfully

applied to the selective separation of glycopeptides and glycoproteins. In order to further improve the density of boronic acid moieties immobilized on  $\text{Fe}_3\text{O}_4$  MNPs, "click chemistry" including CuAAC click reaction<sup>75</sup> and thiol-ene click reaction<sup>83</sup> has been developed for surface modification. The resulting boronate affinity MNPs exhibited a high density (hundreds of mg/g for glycoproteins) and thereby high affinity and excellent selectivity toward glycoproteins were obtained. The greatly enhanced adsorption capacity toward glycoproteins indicated that the 'click' method presents great superiority in ligand immobilization. Unfortunately, the bare MNPs suffer disadvantages such as aggregation and difficult post-modification, which limit their applications in biological systems. To address this issue, core-shell structured magnetic NPs were commonly used in biological separation. Much effort has been made on polymer shell structures owing to their merits including various functional groups, facile post-modification and good biocompatibility. Chen and co-workers<sup>84</sup> fabricated boronic acid functionalized  $\text{Fe}_3\text{O}_4$  hybrid composites for the enrichment of glycoproteins through CuAAC click reaction. The as-prepared  $\text{Fe}_3\text{O}_4$ @poly(4-vinylbenzylchloride)@APBA provided a high surface density of boronate affinity ligands and therefore exhibited large adsorption capacity and remarkable selectivity to glycoproteins at physiological conditions, which was particularly useful for glycoproteomic analysis. However, polymer shell has low mechanical stability and poor resistance to swelling in organic solvents. Thus, silica coating has been widely used as shell of magnetic core to prepare the boronic acid-functionalized core-shell structured  $\text{Fe}_3\text{O}_4$ @ $\text{SiO}_2$  MNPs,<sup>81,82,85</sup> because of its mechanical stability, high hydrophilicity, good solvent resistance to swelling and ease of surface functionalization.

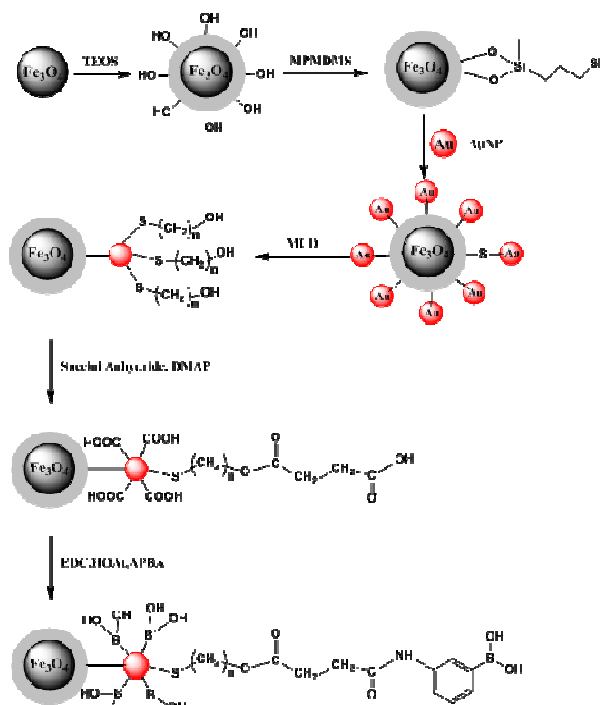


**Fig. 6** The synthetic procedure of the core-satellite-structured composite material. (MPMDMS=3-mercaptopropylmethyl dimethoxy-silane; MUD=11-mercaptoundecanol; DMAP=4-dimethylamionpyridine; EDCI=1-(3-dimethylaminopropyl)-3-ethylcarbodiimide hydrochloride; HOAt=1-hydroxy-7-azabenzotriazole). Adapted from ref. 67 with permission from John Wiley and Sons.

In the past decades, gold NPs have gained increasing attention from analytical chemists due to their easily tuned physical and surface chemical properties, robustness, and high surface areas.<sup>160-162</sup> Because of the nature of gold, the surface of gold NPs could be modified with a large amount of MPBA effortlessly through the robust interaction between the thiol group and gold. As reported by Deng and co-workers,<sup>65,66</sup> MPBA-functionalized gold NPs were successfully applied to the selective separation and enrichment of glycopeptides. In order for rapid separation, magnetic cores are widely employed. However, the dissimilar nature of magnetic core and gold shell becomes a major obstacle in direct coating of MNPs with gold. This issue had been well solved by using the layer-by-layer approach.<sup>163</sup> Deng and co-workers<sup>69</sup> prepared a core-shell nanostructure  $\text{Fe}_3\text{O}_4@\text{C}@\text{Au}$  NPs by layer-by-layer self-assembly. The  $\text{Fe}_3\text{O}_4@\text{C}@\text{Au}$  NPs were used for immobilizing MPBA for the selective enrichment of glycoproteins and glycopeptides. However, this type of boronate affinity NPs may cause strong nonspecific adsorption and severe steric hindrance owing to short spacer arm and therefore reduce the selectivity and affinity. Lu and co-workers<sup>67</sup> fabricated a core-satellite-structured magnetic composite composed of a silica-coated  $\text{Fe}_3\text{O}_4$  “core” and numerous “satellites” of gold NPs with lots of anchor-containing boronic acid (Fig. 6). The anchors could reduce the steric hindrance and suppress nonspecific bindings due to the long spacer arm. This unique composite NPs not only exhibited excellent selectivity, affinity and binding capacity for glycosylated species but also provided fast magnetic recovery. They were successfully employed for the selective enrichment of glycosylated peptides and proteins with even low concentrations. Therefore, all these properties can make this composite material fascinating and promising for high-throughput glycoproteome analysis.

As discussed above, density of functional groups is also one of crucial properties of boronate affinity materials. The higher is the density of ligands, the better the performance the material can provide. In order to significantly increase the density of boronic acid ligand on solid support and thereby provide favourable binding capability and binding capacity, Ye and co-workers<sup>87</sup> developed a nanomaterial of novel structure, polymer brushes containing boronic acid repeating units in flexible polymer chains attached on silica gels using surface-initiated atom transfer radical polymerization (ATRP). Because the composite particles possess a high density of boronic acids appended on flexible polymer chains, the obtained composite nanomaterial showed super high saccharide binding capacity (about 490 mmol/g for fructose) under physiological pH conditions. Moreover, the flexible polymer brushes on silica also enabled fast separation and enrichment of not only simple saccharide but also glycopeptides and glycoproteins. Especially, the flexible polymer brushes with high density of boronic acid ligand significantly improved binding strength toward target glycoproteins due to the synergistic multivalent binding, similar to dendrimer-assisted boronate avidity.

In addition to the above mentioned inorganic NPs, boronate affinity-based organic NPs have been reported by Zhang and co-workers, such as hydrophilic polymer NPs<sup>86</sup> and core-shell polymer NPs.<sup>76</sup> These boronic acid-functionalized NPs could selectively extract glycopeptides and glycoproteins from complex matrix with high-abundance interferents and thus make these materials promising tools for glycoproteomic analysis. However, the uncontrollable polymerization rate may affect the functional monomer amount on the particle surface, resulting in limited binding sites to *cis*-diol-containing molecules. In order to improve the amount of boronic acid immobilized on organic NPs,

they<sup>88</sup> recently synthesized a new type of APBA-functionalized core-shell polymer NPs using a class of controlled/living free radical polymerization, reversible addition-fragmentation chain transfer (RAFT) to form the branched boronate polymer shell. Such superiorly structural boronic acid polymer NPs displayed high binding capacity and good selectivity toward *cis*-diol-containing molecules.

Although all the above mentioned NPs can be used to bind glycopeptides, applications to real samples still remain challenging. First, the sensitivity and selectivity are not quite satisfying because these synthesized materials inevitably cause nonspecific adsorption, especially hydrophobic interaction. As a result, these materials adsorbed a plenty of non-glycopeptides which are dominant in real samples.<sup>62,76</sup> In a typical enrichment procedure, usually three steps are required: incubation, wash, and elution. In the washing step, buffer solutions are used to wash off the nonspecifically adsorbed components, which will cause inevitable loss of target molecules. Especially, in a real-world sample, the target molecules usually exist in very low concentration along with extremely complicated high-abundance interferents. Therefore, it is a great challenge to get sufficient valuable information of glycosylation from real biological samples. In order to overcome this, Lu and co-workers<sup>85</sup> established a novel system based on two different NPs: boronic acid-functionalized  $\text{Fe}_3\text{O}_4@\text{SiO}_2$  core-shell NPs ( $\text{Fe}_3\text{O}_4@\text{SiO}_2$ -APBA) for capturing glycopeptides selectively and poly(methyl methacrylate) (PMMA) nanobeads for strong nonspecific adsorption toward non-glycopeptides. By optimizing the proportion of these two nanomaterials, extremely high sensitivity and selectivity were achieved in analyzing the standard glycopeptides/non-glycopeptides mixture solutions even in a molar ratio of non-glycopeptides/glycopeptides = 100/1. The LOD of this method for glycopeptides was the sub fmol/ $\mu\text{L}$  level. The synergistic method provided excellent selectivity for glycopeptides. Since a washing step was avoided in enrichment operation conditions, the enrichment process was simplified and the recovery efficiency of target glycopeptides reached 90%. Owing to these significant advantages, the established system was successfully applied to analyze human serum with the sample volume as little as 1  $\mu\text{L}$ . All these performances by the synergistic enrichment are much better than employing one enriching material alone.

#### 2.2.4. Molecularly imprinted polymers

Molecularly imprinted polymers (MIPs),<sup>164-168</sup> which are chemical receptors synthesized through polymerization in the presence of a template, have developed into important functional materials with antibody-like binding properties or enzyme-like catalytic activities and found wide applications from sensing to separation to catalysis. Due to the presence of the structure of nanoscale imprinted cavities that are highly complementary to the imprinting molecules, MIPs can provide excellent specificity and high affinity toward target molecules, which is highly favourable for the separation and molecular recognition of analytes in complex samples. In general, there are two types of molecular imprinting methods, covalent imprinting proposed by Wulff<sup>166</sup> and non-covalent imprinting introduced by Mosbach.<sup>169</sup> The non-covalent imprinting method is more flexible concerning the choice of functional monomers and possible target molecules. Another advantage is its simplicity in operation owing to the requirement of only mixing of functional monomers and templates. However, non-covalent imprinting may yield certain heterogeneity of the binding sites owing to the presence of an equilibrium system in prepolymerization complex. In contrast, covalent imprinting protocols yield a more homogeneous

binding-site distribution due to the greater stability of covalent bonds. In addition, the structure of guest-binding site is clearer in covalent imprinting. Because the easy on/off reactivity of boronic acid favours the imprinting and removal of templates, boronic acids have been promising functional monomers for covalent imprinting of *cis*-diol-containing compounds. This significant feature is more advantageous for covalent imprinting of macromolecules than that of small molecules.

Boronate affinity-based molecular imprinting of small molecules was first reported by Wulff and co-workers.<sup>89-91</sup> They prepared a series of boronate affinity-based MIPs using VPBA as the functional monomer for the purpose of constructing chiral cavities as specific receptors. The resulting MIPs exhibited high specificity for the resolution of racemates and thus sort out the isomeric and enantiomer in carbohydrate molecules. Since then, a variety of boronate affinity-based MIPs for small molecules have been reported.<sup>92-102</sup> Karube and co-workers<sup>92</sup> developed a boronate affinity MIP for sialic acid. The polymer showed pH-dependent binding characteristics and exhibited an optimum specificity toward sialic acid at pH 8.1. In order to further enhance the functionality complementary of the imprinted cavities toward template molecules, which can greatly improve the affinity and selectivity of boronate affinity MIPs, Willner and co-workers<sup>94</sup> introduced a non-covalent neutral monomer, acrylamide (AAm) to the boronate affinity molecular imprinting. In this work, a MIP for nucleotide (e.g. adenosine-5'-monophosphate (AMP)) was prepared by copolymerization of AAm with AAPBA. Because AAm can interact with phosphate group and base moieties of nucleotide through hydrogen bonding, the obtained MIP exhibited high specificity and affinity toward the imprinted nucleotide. However, the strong electrostatic repulsion between common boronic acid (e.g. VPBA, AAPBA) and negatively charged analytes (e.g. AMP) can hamper the complexes formation between the boronic acid and AMP to some extent, which is disadvantageous to the formation of boronate affinity MIPs and thus limits the capacities and selectivity of MIPs. To solve this issue, Agrofoglio and co-workers<sup>96</sup> imprinted AMP using VPBA and AAm monomers without incorporating the phosphate group in the selective cavities. In order to obtain AMP-suitable imprinting cavities, an AMP analog was used as the imprinting template, which was formed by replacing the phosphate moiety with the inert group *tert*-butyldimethylsilyl that simulated the steric hindrance. Due to the elimination of the electrostatic repulsion between boronic acid and AMP, selectivity and capacities of the MIPs were improved. Subsequently, they<sup>99</sup> also employed AAm to enhance the functionality complementary of the imprinted cavities toward another template molecule (2,5-deoxyfructosazine). Due to the strong hydrogen bond between AAm and 2,5-deoxyfructosazine, the affinity and selectivity of the MIPs were greatly improved.

However, the use of non-covalent monomers in the covalent imprinting may generate unwanted nonspecific binding sites. Fortunately, the issue can be overcome by a novel boronate affinity-based covalent imprinting strategy, called post-imprinting modification.<sup>95</sup> As shown in Fig. 7, a template-monomer complex was firstly formed before polymerization. After the polymerization, the template was removed from the polymer matrix and then the thiol residues were transformed into sulfonic acid through oxidation (post-imprinted process). In this way, the chemical and structural information of template molecule were well remembered through the fine controlled arrangement of boronic acid and sulfonic acid in the imprinted cavities. Thus, this would create a cavity containing both boronic acid and sulfonic acid residues complementary to dopamine, which avoided the nonspecific binding sites in the MIPs. The obtained MIPs exhibit

enhanced affinity and improved selectivity toward dopamine in aqueous solution via the two-point interaction, i.e. the covalent interaction with boronic acid and electrostatic interaction with the sulfonic acid residue.

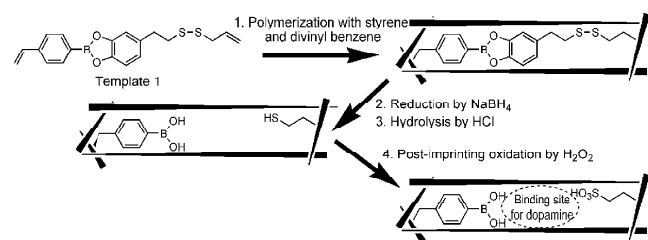


**Fig. 7** Schematic diagram of dopamine imprinting with the post-imprinting oxidation. Reproduced from ref. 95 with permission from The Royal Society of Chemistry.

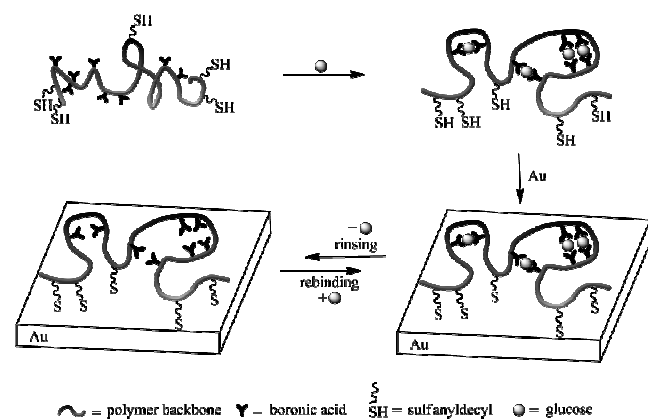


**Fig. 8** Schematic representation of the solution-to-surface imprinting process based on the conformational changes of boronic-acid-appended poly(L-lysine) derivative in the presence of D-glucose. Adapted from ref. 93 with permission from John Wiley and Sons.

In many situations, template, functional monomers and crosslinker were mixed together and the mixture was polymerized into a polymer. After that, the polymer obtained by bulk polymerization has to be crushed, ground and sieved to an appropriate size. Such an imprinting methodology is called bulk imprinting. Technically, bulk imprinting is relatively simple. It had been widely used in the early stage of molecular imprinting and it is still in use. However, it suffers apparent disadvantages, such as incomplete template removal, time-consuming, small binding capacity, and slow mass transfer. These drawbacks apparently hinder wide applications of bulk imprinting. To address these issues, Shi and co-workers<sup>101</sup> deposited an imprinting layer formed through copolymerization of AAm and EDMA in the presence of template (dopamine) onto the surface of APBA-functionalized poly(aniline-co-anthranilic acid). Because of the obtained surface-situated template-imprinted sites, the MIPs provided more surface binding sites and fast association kinetics. Shinkai and co-workers<sup>93</sup> developed a method called solution-to-surface molecular imprinting. It based on the conformational changes of boronic acid-appended poly(L-lysine) in the presence of the template. As shown in Fig. 8, the binding of D-glucose with two boronic acid moieties of a polypeptide chain caused conformational changes of the polypeptide chain, thus forming intrapolymeric cross-links. After that, the formed polymer-template complex was anchored onto a metal surface (such as Au) to fix the conformation of the polypeptide. After



removing the template molecules by rinse, a glucose-selective molecularly imprinted monolayer was formed. In comparison with traditional polymer imprinting, this approach ensured more homogeneous binding sites and quantitative template removal, and therefore provided high specificity and high imprinting efficiency. However, this strategy is not suitable to imprint single *cis*-diol group-containing compounds such as fructose.

As compared with the imprinting of small molecules, the imprinting of water-soluble biomacromolecules especially proteins is rather challenging. One reason is that the large size of proteins makes it difficult to be removed from highly cross-linked polymer networks. The other is that conformational change of proteins may occur under harsh polymerization conditions. Considering these, many approaches have been proposed, such as surface imprinting,<sup>170,171</sup> epitope imprinting,<sup>172,173</sup> Pickering emulsions,<sup>174</sup> metal coordination,<sup>175</sup> hierarchical imprinting,<sup>176</sup> and so on. Among the strategies used for protein imprinting, surface imprinting is the most popular method, which can solve the problem of diffusion limitation caused by large size of protein. Based on surface imprinting, several techniques have been developed, such as surface initiated polymerization<sup>177,178</sup> and immobilized template-based imprinting.<sup>171,179</sup>

The covalent imprinting of glycoproteins using boronic acids as functional monomers first appeared in 1985. Mosbach and co-workers<sup>103</sup> prepared transferrin-imprinted polysiloxane-coated silica. However, covalent imprinting of other glycoproteins with similar approach had not been successfully demonstrated owing to problems such as protein precipitation. Until recently, several boronate affinity-based glycoprotein-imprinted polymers were developed using surface initiated polymerization.<sup>104,108</sup> Liu and co-workers<sup>104</sup> developed a general and facile approach for preparing MIPs for glycoproteins, namely, photolithographic boronate affinity molecular imprinting. As shown in Fig. 9, the principle relied on UV-initiated free radical polymerization between a cross-linker (such as polyethylene glycol diacrylate (PEGDA)) and a functional monomer (such as VPBA). The template was first mixed with the monomer in an appropriate porogen solution of pH  $\geq 8.0$ . The template and the monomer self-assembled into a covalent complex owing to boronate affinity binding. Mixing of the complex with the cross-linker and an appropriate UV initiator yielded a prepolymer solution. Through UV curing for a short period (tens of seconds), the prepolymer quickly polymerized into a polymer. To make molecularly imprinted thin-layer arrays, the pre-polymer solution was first cast onto the surface of a solid substrate, such as a glass slide or a filter membrane. The imprinted template in the MIP can be easily removed with an acidic solution, leaving cavities complementary to the 3D shape of the template. The prepared boronate MIP arrays provided several highly attractive features such as high affinity (the  $K_d$  value was 85 nM), high specificity (cross-reactivity  $\leq 8.8\%$ ), superb tolerance for interference (allowed for the presence of competing monosaccharide at a one million-fold higher concentration) and the applicability to a wide range of sample pH values (5.0-9.0). Owing to these advantages, glycoprotein-imprinted microarrays prepared by this method have been used as substitutes of antibodies for enzyme-linked immunosorbent assay (ELISA) of trace  $\alpha$ -fetoprotein (AFP) in human serum. However, this imprinting approach is applicable only to substrates that can accept UV radiation.

The strategy of using template immobilization has been used to develop a series of boronate affinity-based MIPs.<sup>105-107,109-112</sup> Materials of various formats have been used as solid substrates, such as magnetic  $\text{Fe}_3\text{O}_4@Au$  nanofibers,<sup>105</sup> polymer nanospheres,<sup>106</sup> macroporous monoliths,<sup>107,109</sup> glass slide,<sup>109</sup> 96-well microplate,<sup>110,111</sup> and silica NPs.<sup>112</sup> On the other hand, the

controllability and hydrophilic nature of the imprinting coating are critical for the binding properties of the prepared MIPs. To date, a series of monomers have been introduced for the preparation of imprinting coatings, such as acrylamide, dopamine, siloxane, aniline, and so on.

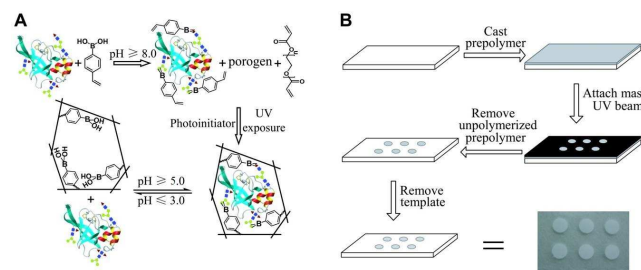


**Fig. 9** The principle (A) and procedure (B) of photolithographic boronate affinity molecular imprinting. Adapted from ref. 104 with permission from John Wiley and Sons. (The pH for rebinding is adjusted to  $\geq 5.0$  according to the text of ref. 104).

Chen and co-workers reported the first example of template immobilization-based boronate affinity surface imprinting by using magnetic  $\text{Fe}_3\text{O}_4@Au$  multifunctional nanofibers as substrate.<sup>105</sup> In the imprinting process, AAm and MBAA were used to prepare the imprinting layer. The resultant MIPs showed good selectivity and rational binding kinetics to target glycoprotein. Besides, Li and co-workers<sup>106</sup> reported MMA-VPBA based polymer nanospheres for template immobilization using poly(AAm-co-MBAA) as the imprinting layer. Due to the remarkable biocompatibility and easy synthesis of this polymeric material, the resulting MIPs exhibited high adsorption capacity and good specificity toward the template glycoprotein. In recent years, protein-imprinted monolithic columns have attracted increasing attention due to significant advantages monolithic column features. Lin and co-workers<sup>107</sup> developed boronate affinity-based surface imprinted monolithic columns by employing polydopamine as the imprinting coating. An imprinting factor of 2.76 was achieved. As a monolithic column is a highly cross-linked 3D continuous porous polymer, it is more challenging to prepare molecularly imprinted monolithic columns for proteins. Using monolithic columns as the imprinting substrates, the surface imprinting approach provides superiority over the other imprinting approaches.

Although the above mentioned imprinting approaches have demonstrated potential applicability of boronate affinity-based surface imprinting, the merits of this strategy are still in vague and the properties of the prepared MIPs have not been soundly explored. Liu and co-workers<sup>109</sup> reported a general and facile approach, called boronate affinity-based controllable oriented surface imprinting, for efficient imprinting of glycoproteins. Fig. 10 depicts a schematic diagram of this imprinting strategy. The process involved several consecutive steps. First, a boronic acid-functionalized solid substrate was prepared and then a target glycoprotein was immobilized onto the substrate surface by virtue of the boronate affinity. After a hydrophilic coating formed by in-water self-copolymerization of monomers was deposited onto the substrate surface, the glycoprotein was removed by disrupting the boronate affinity binding with an acidic solution, thus 3D cavities complementary to the molecular size and shape of the template were well formed in the imprinting layer. The thickness of the imprinting layer linearly increased as increasing the imprinting time, which provided a straightforward way to precisely control the thickness. In order to achieve good performance, the thickness of the imprinting layer was adjusted to 1/3 to 2/3 of the

molecular size of the template in one of the three dimensions. Dopamine and APBA were chosen as dual monomers and their copolymerized product with 1:1 molar ratio was used as an imprinting coating. This was mainly because this dual monomer system could provide the most favourable properties. If dopamine is used alone, it will compete with and replace glycoprotein templates so that the imprinting will not obey oriented imprinting fashion. While if APBA is used alone, the resultant polymer may contain some residual boronic acid moieties so that non-imprinting binding sites are present outside of the imprinted cavities. To eliminate residual boronic acid groups in poly(APBA-co-dopamine) polymer, the molar ratio between APBA and dopamine was set at 1:1.

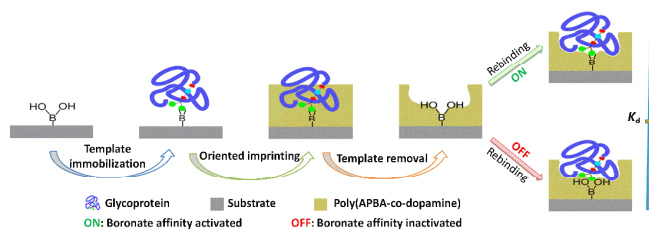


**Fig. 10** Schematic diagram of boronate affinity-based controllable oriented surface imprinting of glycoproteins. Reproduced from ref. 109 with permission from The Royal Society of Chemistry.

As compared with the photolithographic boronate affinity molecular imprinting approach,<sup>104</sup> an obvious advantage of the boronate affinity-based controllable oriented surface imprinting is that it is applicable to wider range of substrate formats. Imprinting on glass slide and monolithic column had been well demonstrated. As compared with boronate affinity-based bulk imprinting and the other surface imprinting, this imprinting strategy is extremely favourable to the template removal. As compared to the result Lin and co-workers reported,<sup>107</sup> the imprinting factor increased from 2.76 to 4.60. The imprinting efficiency was 48.5%, which is also higher than a previously reported value (41%).<sup>104</sup> Such a high imprinting efficiency benefits from the boronate affinity-based oriented surface imprinting. The prepared MIP exhibited strong affinity toward glycoproteins (with a dissociation constant of 1.2 nM for HRP at pH 7.4).

Moreover, a unique affinity-tunable dual-mode binding mechanism was observed for the boronate affinity-based MIPs: high affinity mode (boronate affinity interaction is on) and low affinity mode (boronate affinity interaction is off), allowing this affinity-tunable material for even wider applications. This unique mechanism was disclosed for the first time. It provides not only a unique possibility to adjust the binding strength while keeping the specificity but also new insights into the roles of affinity-determining factors in molecular imprinting. The cavities well fabricated can rebind with template molecules even when there are no apparent interactions between the template molecules and the functional moieties on the cavities. This very much changed the common understanding about the molecular interactions required for MIPs; that is, either multiple weak interactions as required by non-covalent imprinting or number-limited but strong interactions as required by covalent imprinting.

Overall, MIPs prepared by the boronate affinity-based controllable oriented surface imprinting approach exhibits several highly favourable features over existing methods, such as excellent specificity, high imprinting efficiency, controllable binding mode, fast equilibrium kinetics and widely applicable substrates (from 2D to 3D, from regular size to nanoscale).

To prepare MIPs for use in high throughput clinically diagnostic applications, Liu and co-workers<sup>110,111</sup> extended the above imprinting approach to 96-well microplates, which was the most commonly used platform for high throughput ELISA analysis of disease biomarkers in clinical diagnostics. In the imprinting process, a hydrophilic coating with appropriate thickness formed by in-water self-polymerization of aniline was used as the imprinting layer. AFP or alkaline phosphatase (ALP)-imprinted 96-well microplates exhibited strong binding affinity toward the template molecules and the dissociation constant reached the nM level, which was comparable to that of real antibodies (usually  $10^{-7}$ – $10^{-9}$  M). The high binding strength led to a lower binding pH of the boronate affinity-based MIPs, which is particularly advantageous for real sample applications. The fabricated glycoprotein-imprinted microplates can be well used as substitutes of antibody-coated microplates for ELISA of trace glycoproteins in complex samples such as human serum.

Owing to its remarkable advantages as mentioned earlier, silica based material is an ideal candidate as imprinting substrate and imprinting layer. As reported by Lin and workers,<sup>112</sup> boronic acid-functionalized silica NPs and thin layer formed by the polycondensation of 3-aminopropyltriethoxysilane (APTES) and *n*-octyltrimethoxysilane (OTMS) were used as the imprinting substrate and imprinting coating, respectively. The corresponding imprinting factor reached 2.71.

### 2.2.5. Temperature-responsive materials

Stimuli responsive materials can be used for a variety of applications such as tunable catalysis, drug delivery, self-healing coating and bioseparation. The interests to these materials have significantly increased due to their promising potential. Among them, pH and temperature responsive materials have been considerably investigated because they are convenient and effective stimuli in many applications. Boronate affinity materials are one of typical pH responsive materials because of its pH-controlled capture/release of *cis*-diol-containing molecules. In addition, temperature responsive materials also gained increasing attentions for their wide applications in separation science and biomedicine.<sup>180-182</sup> Poly(*N*-isopropylacrylamide) (poly(NIPAAm)) is the most well-known temperature-responsive polymer with a lower critical solution temperature (LCST) (32°C in the pure water).<sup>183,184</sup> Polymers of this type undergo a thermally induced, reversible phase transition and they are soluble in a solvent (water) at low temperatures but become insoluble as the temperature increases above the LCST (hydrophilic/hydrophobic property alteration). Boronic acid-containing poly(NIPAAm) can also show temperature-sensitivity properties.<sup>113-121</sup> At low temperature (below LCST), the polymer chains are in the form of extended random coils and are hydrophilic. In this status, the boronic acid groups are mainly dissociated and are in the tetrahedral anionic form at appropriate pH conditions, which form stable cyclic esters with *cis*-diol-containing compounds. When the temperature increases above the LCST, the polymer chains exist in the form of collapsed globules and are hydrophobic, which may lead to a reduced local permittivity around the phenylboronic acid moieties.<sup>185,186</sup> As a result, the  $pK_a$  of boronic acid is increased with a temperature rises and therefore causes temperature-induced release of *cis*-diol-containing compounds. Moreover, the conformational changes of the polymer chains from a flexible state to a rigid state with rising temperature may give rise to the steric hindrance that restricts the interaction between boronic acids and *cis*-diol groups.<sup>114</sup> Therefore, capture and release of *cis*-diol-containing biomolecules using boronic acid-containing poly(NIPAAm) can be also realized by the temperature-controlled fashion.

The most widely used synthesis approach is the copolymerization of NIPAAm and boronic acid such as VPBA or AAPBA.<sup>114-116,118,120,121</sup> Deng and co-workers<sup>118</sup> designed and prepared a temperature-responsive boronate affinity material for chromatographic separation by grafting poly(NIPAAm-co-VPBA) onto the surface of silica microspheres via ATRP. As depicted in Fig. 11, a column packed with the poly(NIPAAm-co-VPBA) grafted silica microspheres exhibited specific capture/release of *cis*-diol-containing biomolecules through adjusting only the temperature. However, a complex temperature control device is needed for the temperature-controlled binding/elution process. Because microfluidic devices have several advantages including less reagent consumption, quick response time, and high throughput, two types of microfluidic chips with temperature-responsive boronate affinity were fabricated by grafting poly(NIPAAm-co-VPBA)<sup>120</sup> and poly(NIPAAm-co-AAPBA)<sup>121</sup> onto glass substrates and polydimethylsiloxane, respectively. The two prepared microfluidic chips were successfully used to selectively capture and release *cis*-diol-containing biomolecules such as adenosine by temperature-modulated changes. Furthermore, Tuncel and co-workers<sup>114</sup> prepared temperature-responsive poly(NIPAAm-co-VPBA) latex particles by dispersion polymerization. The particles exhibited good adsorption/desorption of nucleotides and nucleic acids via temperature-responsive switch.

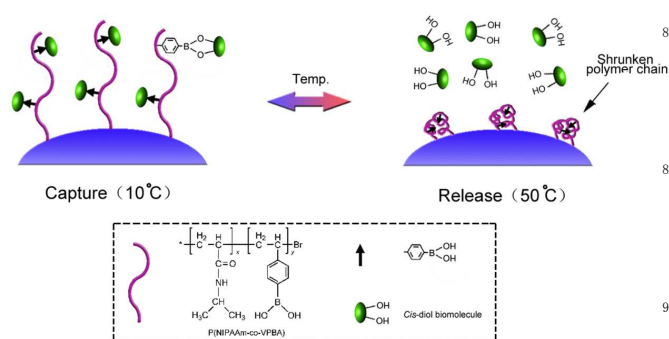


**Fig. 11** Schematic illustration of the thermally modulated capture and release of *cis*-diol-containing compounds on the poly(NIPAAm-co-VPBA) grafted silica surface. Reproduced from ref. 118 with permission from The Royal Society of Chemistry.

Alternatively, boronic acid functional groups can be grafted onto the poly(NIPAAm) networks.<sup>113,119</sup> Ye and co-workers<sup>119</sup> developed a boronic acid terminated temperature-responsive poly(NIPAAm) polymer through CuAAC reaction. At physiological pH, the polymer architecture could effectively capture a *cis*-diol-containing compound at low temperature, which was separated from aqueous solution by increasing the temperature above the LCST.

### 2.2.6. Nanoconfining affinity materials

Confinement effect has attracted enormous attention, from physics to chemistry to material science. Nanoconfinement effect often occurs in advanced materials such as nanomaterials,<sup>187</sup> mesoporous materials,<sup>188</sup> porous materials.<sup>189</sup> It's interesting to note that several of the above mentioned boronate affinity porous materials especially molecularly imprinted materials showed high selectivity and high affinity toward target molecules. Particularly, as suggested by the above mentioned affinity-tunable dual-mode binding mechanism of boronate affinity MIPs, cavities well fabricated can rebind with template molecules even when there

are no apparent interactions between the template molecules and the functional moieties on the cavities. In another word, the confinement effect of the nanoscale imprinting cavities could predominantly determine the overall binding strength of the MIPs toward the target molecules. However, a sound understanding of this phenomenon was lacking. Recently, Liu and co-workers<sup>190</sup> presented a quantitative study on the effect of nanoscale spatial confinement on molecular interactions. Based on a model host material, boronic acid functionalized MCM-41 silica, the enhancement of binding strength was found to strongly depend on the difference between the molecule size and the pore size. The smaller the difference, the larger was the enhancement. In this work, enhancement by a factor as much as 3 orders of magnitude was observed. This unveiled the origination of the highly favourable affinity properties of molecularly imprinted materials. These understandings are extremely important for the rational design of advanced functional materials for emerging applications.

Inspired by the above mentioned merits of confinement effect, by employing nanoconfinement effect as the core element, Liu and co-workers developed a novel type of functional material, called nanoconfining affinity material (NCAMs).<sup>122</sup> The initiative of this type of material was also inspired by the pH-responsive capture/release pattern of boronate affinity materials. The affinity of NCAMs arose from not only the interactions between the functional groups and molecules but also their porous structure. Two NCAMs were designed to have the pores with the size range from 3 to 30 nm, which are comparable to the molecular size of the most frequently encountered proteins. The NCAMs were modified with *N*-( $\beta$ -hydroxy propyl)ethylene diamine (HPEDA), which provided a boronate affinity-like pH-controlled capture/release pattern. The NCAMs were able to bind proteins with a molecular mass larger than 18 kDa. Different from boronate affinity materials, which only allow for selective capture/release of glycoproteins, applicable targets of the NCAMs covered not only glycoproteins but also non-glycoproteins. The dissociation constants ranged from  $10^{-5}$  to  $10^{-7}$  M, which were lower than those of conventional boronate affinity materials. With these unique binding properties, promising applications such as chiral separation, immobilized enzyme reactors and depletion of high-abundance serum proteins were well demonstrated.

Very recently, Liu and co-workers<sup>191</sup> employed boronic acid functionalized mesoporous silica (MCM-41) as a selective extraction sorbent and nanoscale reactor for solid phase saccharide labeling. Owing to the nanoconfinement effect derived from the highly ordered mesoporous structure, the solid-phase labeling approach provided several advantageous features, including faster reaction speed (only taken 2 min), high product purity and much lower applicable saccharide concentration ( $10^{-9}$  M, four orders of magnitude lower than that of liquid-phase labeling). This approach opened up new avenues to the facile and efficient labeling of saccharides and can be a promising approach for important applications such as glycomics. Besides, the application of mesoporous materials as nanoreactors can be expanded to other solid-phase reactions.

## 3. Applications

Although it has been already more than 40 years since boronate affinity material first appeared in 1970, boronate affinity materials had not found wide applications before 2006. Boronate affinity materials have gained rapid and deep development over

the last decade. Particularly, a variety of boronate affinity materials with desirable properties, such as low binding pH, high binding affinity and good selectivity, have been prepared within this period. The desirable properties enabled various important applications, such as affinity separation/enrichment, proteomics, metabolomics, disease diagnostics and aptamer selection.

### 3.1. Affinity separation

Boronate affinity materials have been widely used as selective sorbents for affinity separation of *cis*-diol-containing biomolecules in real complex samples, such as egg white,<sup>43,48,75,81,83,84,86</sup> human serum,<sup>45,82,109,112</sup> and human saliva.<sup>56,60,80</sup> Boronic acid-functionalized Fe<sub>3</sub>O<sub>4</sub> MNPs and Fe<sub>3</sub>O<sub>4</sub> hybrid composites have been used to capture glycoproteins from a fresh egg white sample.<sup>75,81,83,84</sup> Chen and co-workers<sup>75,83,84</sup> isolated glycoproteins directly from the egg white by using high-capacity boronic acid-functionalized Fe<sub>3</sub>O<sub>4</sub> MNPs. According to the sodium dodecyl sulfate polyacrylamide gel electrophoresis (SDS-PAGE) analysis, the bands of OVA (46 kDa, 54%), ovotransferrin (76.7 kDa, 12%), ovoinhibitor (49 kDa, 1.5%), and lysozyme (14.4 kDa, 3.4%) appeared in the diluted egg white without treatment using the MNPs, among which the former three are glycoproteins. After egg white samples were treated by the MNPs, only the bands of the three glycoproteins faded, while the band of lysozyme remained unchanged. The result indicated that the boronic acid-functionalized MNPs have excellent practicability for affinity separation of glycoproteins from the egg white. Although the boronate affinity MNPs allow for easy magnetic separation, they are not suitable for online operation and very minute sample volume. Monodisperse boronate polymer NPs<sup>86</sup> and boronate affinity monoliths<sup>43,48</sup> were also successfully employed for the isolation and enrichment of glycoproteins from egg white. The above mentioned materials provided only class-selectivity and thereby failed to extract a specific compound from complicated samples.

Owing to their high specificity, boronate affinity MIPs allowed for specific extraction of glycoproteins from complicated samples. HRP-imprinted silica NPs have been used for specific extraction of HRP from a diluted human serum spiked with HRP.<sup>112</sup> SDS-PAGE experiments indicated that in spite of the presence of a large variety of high-abundance non-glycoproteins (e.g. human serum albumin (HSA)) and glycoproteins (e.g. IgG, transferrin (TRF)) in human serum, most HRP (75.6%) in human serum was successfully extracted by the HRP-imprinted silica NPs. Liu and co-workers<sup>109</sup> prepared a TRF-imprinted monolithic capillary and used it for specific extraction of TRF from human serum. According to matrix-assisted laser desorption/ionization time-of-flight mass spectrometry (MALDI-TOF MS) analysis, only TRF was extracted from the human serum by the TRF-imprinted monolithic capillary. These results well demonstrated the feasibility of boronate affinity MIPs for affinity separation of glycoproteins in complex real samples.

Antibodies are molecular workhorses in biological research, disease treatment and diagnostics. The use of monoclonal antibodies as effective therapeutics for cancer, autoimmune, inflammation and infectious diseases generates tens of billions dollar annual market. Purity is a critical prerequisite for antibody applications. Protein A-based affinity chromatography has been the gold standard for antibody purification. However, protein A is associated with apparent disadvantages, including high cost, poor stability and harsh product release conditions. Liu and co-workers<sup>110</sup> developed a restricted access boronate affinity porous monolith with protein A-like specificity.<sup>45</sup> As shown in Fig. 12, this biomimetic material allowed for specific extraction of IgG from human serum. If this material could be effectively scaled up, it

would be of high economic value. However, difficulty in precise pore size control may hinder large scale production.

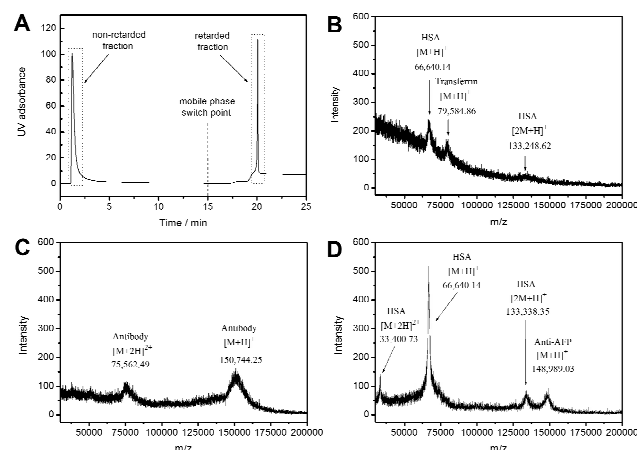


**Fig. 12** Fractionation of human serum sample by boronate affinity chromatography on the restricted access boronate affinity monolithic capillary (A) and MALDI-TOF MS spectrum for the non-retarded (B), the retarded fraction (C) and the standard mixture of HSA and anti-AFP antibody (D). Adapted from ref. 45 with permission from The Royal Society of Chemistry.

As many glycoproteins of interest usually exist in very low abundance along with high-abundance interfering components such as sugars and non-glycoproteins in human saliva, highly efficient affinity separation and enrichment is a critical step for the analysis of glycoproteins. Boronate affinity materials such as 3-carboxybenzoboroxole-functionalized monolithic column,<sup>56</sup> boronate avidity MNPs,<sup>80</sup> and boronate avidity monolithic capillary<sup>60</sup> have been successfully applied to the selective capture or enrichment of trace glycoproteins from human saliva.

### 3.2. Proteomics

A proteome is the entire set of proteins expressed by the genome in an organism or a biological system. Its complexity is further increased due to the presence of post-translational modifications of proteins. Protein glycosylation has been recognized as one of the most popular post-translational modifications. In almost all glycoproteins, the carbohydrate units are attached to the protein backbone either by N- or O-glycosidic bonds or by both types of linkage. Among these types of glycosylation, N-glycosylation is widely distributed in organisms with the  $\beta$ -glycosylamine linkage of N-acetylglucosamine (GlcNAc) to asparagine. Protein glycosylation plays essential roles in many biological processes, such as molecular recognition, inter- and intracellular signaling, immune response and so on.<sup>192</sup> In addition, the changes in glycoprotein abundance, glycosylation degree, and glycan structure are associated with a variety of diseases. A lot of glycoproteins, such as prostate-specific antigen (PSA), AFP, carcinoembryonic antigen (CEA), have been used as disease biomarkers and therapeutic targets.<sup>193,194</sup> The study of glycoproteomics, which mainly focus on the identification of glycosylation sites, glycan structure analysis, site occupancy, glycan isoform distribution and quantitative analysis of the glycoproteome, has become a popular research topic, and is quickly emerging as an important technique for biomarker discovery. MS is a key analytical technique in proteomic researches since MS can provide both structural and quantitative information. However, the study on protein glycosylation in proteomes has confronted a great challenge. This is mainly due to



that glycopeptides have relatively low abundance and their ionization efficiency is much lower compared with non-glycopeptides and thereby the mass spectrometric response of glycopeptides can be significantly suppressed by high-abundance non-glycopeptides. Therefore, highly efficient enrichment strategies are required to isolate and enrich glycoproteins/glycopeptides prior to MS analysis. To date, lectin<sup>195,196</sup> and hydrazine chemistry<sup>197,198</sup> are the most commonly used methods for the selective enrichment of glycopeptides/glycoproteins from complex samples. However, a certain lectin can bind only a narrow range of glycopeptides/glycoproteins and therefore multiple lectins have to be used for comprehensive glycoproteome analysis. Although the hydrazine chemistry-based method is effective for the identification of a lot of glycopeptides from complex samples, it involves multiple chemical derivatization steps. Since boronic acids can bind *cis*-diol-containing structures, which present in most sugar moieties, boronate affinity materials are particularly beneficial for glycoproteomic studies.

A large number of boronate affinity materials have been used for the selective isolation and enrichment of glycopeptides from standard glycoprotein digests.<sup>34,36,61,64,66,69-71,76,199</sup> Boronic acid-functionalized FDU-12 mesoporous silica was used to enrich glycopeptides from HRP tryptic digests which contain glycopeptides and non-glycopeptides.<sup>61</sup> MALDI-TOF-MS analysis indicated that 5 glycopeptides were successfully enriched and identified. The detected number of glycopeptides was a little low, which is probably due to narrow pore size distribution of the mesoporous silica. Deng and co-workers<sup>69</sup> applied boronic acid-functionalized core-shell Fe<sub>3</sub>O<sub>4</sub>@C@Au NPs to treat the tryptic digests of HRP. Based on MALDI-TOF-MS analysis, 13 glycopeptides were detected. Zhang and co-workers<sup>76</sup> later employed boronic acid-functionalized core-shell polymer NPs to enrich glycopeptides from HRP digest. Owing to the improved yield of boronic acid modified on the polymer NPs, totally 18 glycopeptides were captured by the NPs and then identified by MALDI-TOF-MS for HRP digests. Boronate affinity monolithic columns were also applied to selectively enrich glycopeptides from HRP digests. A poly (AAPBA-co-EDMA) monolithic column<sup>34</sup> was used for affinity enrichment. A total of 10 glycopeptides were enriched by this column and then detected by MALDI-TOF MS. As a relatively hydrophobic cross-linker (EDMA) was used, the hydrophobicity of the prepared column might be a unfavourable factor that may affect the selectivity to some extent. Liu and co-workers<sup>56</sup> recently employed a highly hydrophilic 3-carboxybenzoboroxole-functionalized monolithic column to selectively enrich glycopeptides from the tryptic digests of HRP followed by MALDI-TOF-MS analysis. Totally 22 glycopeptides were effectively enriched and identified. The number of the identified glycopeptides is the highest among all boronate affinity extraction-based MS analyses. This was attributed to the excellent selectivity and affinity of the monolithic column.

All above mentioned strategies need eluting step and sample transfer for further analysis, which causes longer time consumption and may lead to sample loss. To isolate and enrich glycopeptides for direct MS analysis, boronic acid-functionalized gold-coated stainless steel and gold-coated Si wafer have been prepared as MALDI plates.<sup>65,199</sup> This on-plate strategy can avoid the indispensable eluting step and sample transfer due to the combination of selective enrichment and direct detection on the target plate, and thus preventing possible sample loss and allowing for the integration of analytical procedures. This on-plate enrichment strategy provided several advantages, including relatively small amount of sample needed, low detection limit,

and rapid selective enrichment. It is promising for high-throughput glycoproteomic research. Totally 12 and 16 glycopeptides were found after treating the tryptic digests of HRP with the boronic acid functionalized gold-coated stainless steel and boronic acid functionalized gold-coated Si wafer, respectively. The LOD reached the fmol/μL level.

Glycoproteomics analysis of real samples is more challenging as compared with the identification of glycosylation with glycoprotein standards, which have attracted increasing attention in recent years.<sup>62,67,79,85,200,201</sup> A boronic acid-functionalized mesoporous silica was applied to enrich endogenous glycopeptides from rat serum.<sup>62</sup> Through nano-LC-MS/MS analysis, 15 glycopeptides and their 15 corresponding glycosylation sites were identified, which were all newly discovered. However, the presence of glycopeptides/non-glycopeptides-suitable pore size may cause strong non-specific adsorption. This might be a main reason why mesoporous silica has not been widely applied to glycoproteomics analysis of real samples. Besides, Yang and co-workers<sup>79</sup> developed a boronic acid-functionalized detonation nanodiamond for the specific enrichment of glycopeptides from mouse liver. The nanodiamond showed good dispersibility in aqueous solution and had plentiful boronic acid functional groups on the surface. It allowed for efficient enrichment of glycoproteins from mouse liver sample. Using the combination of the boronate affinity enrichment with liquid chromatography-electrospray ionization MS (LC-ESI MS), 35 glycosylation sites (40 different N-glycosylation peptides) within 34 unique glycoproteins were identified. Among these identified glycosylation sites, 24 sites were newly identified.

In addition, Lu and co-workers<sup>67</sup> successfully applied boronic acid-functionalized core-satellite composite NPs to human colorectal cancer tissues. Proteins extracted from human colorectal cancer tissues were first incubated with the composite NPs. The extracted glycoproteins were then digested by trypsin and deglycosylated by PNGase F sequentially. The peptide mixture was subjected to automated 2D LC-MS/MS analysis. In all, 194 N-linked glycosylation sites (190 unique glycopeptides) mapped to 155 different glycoproteins were identified and 85.1% (165 sites) of them were discovered for the first time. Apparently, the highly efficient boronate affinity core-satellite composite NPs exhibited good performance. If APBA is replaced by a high-performance boronate ligand, such as DFFPBA or 3-carboxybenzoboroxole, the resulting boronic acid-functionalized core-satellite composite NPs may provide better results.

Non-enzymatic glycation of peptides and proteins by D-glucose has important implications in the pathogenesis of diabetes mellitus, especially in the development of diabetic complications. In order to find more sensitive and informative protein biomarkers for monitoring of glycemic control and to better understand the role of glycation in the development of diabetic complications, comprehensive proteomic studies are required to identify glycated proteins whose altered structure may be related to pathology. Based on the hyphenation of boronate affinity gel column with LC-MS/MS, Metz and co-workers<sup>201</sup> developed a system for the analysis of glycated peptides and proteins in human serum. The boronate affinity enrichment was carried out at two level; first on the protein level and then on the peptide level. A total of 88 unique glycated peptides and corresponding 27 unique glycoproteins were identified. Up to 87.6% of all peptides were identified as glycated peptides in samples subjected to the dual enrichment. In contrast, 76.4% of all peptides were identified as glycated in samples enriched on only the peptide level. Only 12.3% of all peptides were identified as glycated in samples enriched on only the protein level. Without enrichment, only 6.4% of all peptides were identified as

glycated. Therefore, the dual enrichment on both the protein and peptide level using the boronate affinity gel column exhibited more efficient identification of glycated peptides. Although conventional boronate affinity gel columns have been used in glycoproteomic studies, they cannot meet the requirement of fast and nanoliter scale analysis in modern x-omics due to the poor mechanical stability. Lu and co-workers<sup>85</sup> recently proposed a synergistic enrichment strategy, which combined  $\text{Fe}_3\text{O}_4@/\text{SiO}_2$ -APBA and PMMA as selective sorbents for the enrichment of glycopeptides from the tryptic digests of human serum, followed by MALDI-TOF MS analysis. The principle of the synergistic enrichment strategy is shown in Fig. 13. Proteins extracted from human serum were first digested with trypsin and incubated with the two kinds of NPs. After that, the eluted glycopeptides were deglycosylated by PNGase F and the deglycosylated peptides were subjected to nano-LC-MS/MS analyses. A total of 147 different N-glycosylation peptides with corresponding 153 glycosylation sites within 66 unique glycoproteins were identified. In contrast, only 95 glycopeptides with corresponding 101 glycosylation sites were identified mapped to 44 glycoproteins by  $\text{Fe}_3\text{O}_4@/\text{SiO}_2$ -APBA alone. The synergistic enrichment strategy provided apparent merits over conventional single enrichment strategy for the identification of glycopeptides/glycoproteins in real biological samples. As human saliva is rich in N-glycoproteins, identification of salivary N-glycoproteins, their glycosylation sites and the glycans structures are of increasing interest for clinical applications. Schulz and co-workers<sup>200</sup> developed a method combining boronic acid-based glycoprotein enrichment and MS detection to identify N-glycosylation sites in human saliva. In a saliva sample digested with trypsin, 46 N-glycosylation sites in 40 peptides were identified; while in a sample digested with AspN, 39 N-glycosylation sites were identified from 49 peptides. Combining the results from the two aspects, a total of 67 independent glycosylation sites from 24 unique proteins were identified, which was 3.9-fold more as compared with unenriched saliva. With this approach, quantification of glycosylation site occupancy was evaluated. Among the 21 measured glycosylation sites, 15 sites were completely glycosylated with an occupancy of 100%. The other 6 glycosylation sites were measured with an occupancy of less than 100%. Clearly, using the combinational digested approach of trypsin and AspN, more glycosylation sites can be identified than using single digested approach. If these boronate affinity materials used for glycoprotein enrichment are replaced by high-performance boronate affinity materials, more appealing results may be accomplished.

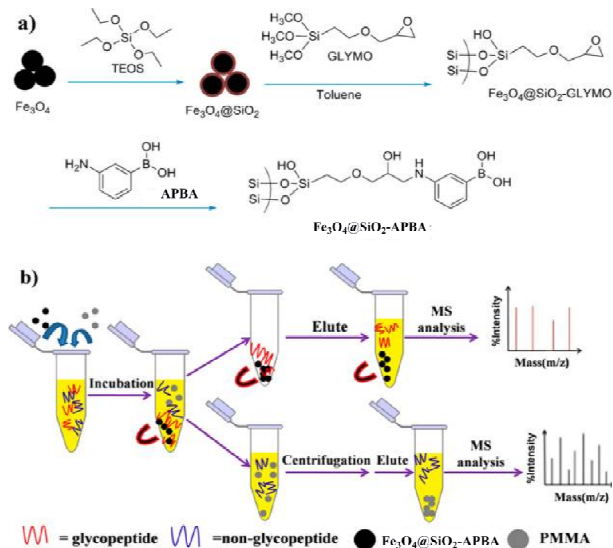


**Fig. 13** Schematic illustration of the (a) synthetic procedure for the  $\text{Fe}_3\text{O}_4@/\text{SiO}_2$ -APBA nanoparticles and the (b) synergistic enrichment process for the glycopeptides using  $\text{Fe}_3\text{O}_4@/\text{SiO}_2$ -APBA nanoparticles and PMMA nanoparticles. Adapted from ref. 85 with permission from American Chemical Society.

### 3.3. Metabolomics

Metabolomics is a comprehensive tool for monitoring the metabolic processes within biological systems and can be widely applied to the determination of diagnostic biomarkers for certain diseases or treatment outcomes.<sup>202,203</sup> Especially, there is great potential for metabolomics to be implemented in cancer research because cancer may modify metabolic pathways in the whole organism. Ribosylated metabolites, especially urinary modified nucleosides can provide detailed information about the progression of a pathological process and have been suggested as biomarkers for early cancer diagnostics.<sup>204,205</sup> High interest in metabolomics and the important role of nucleosides as cancer markers result in the increased analytical needs in the separation, determination and identification of a large number of nucleosides in biological samples. As boronate affinity materials can be used to effectively isolate and enrich nucleosides from biological samples due to the vicinal hydroxyl groups contained in the structure of nucleosides, further analysis and identification of nucleosides can be achieved.

Liu and co-workers<sup>41,46,47,52,57</sup> have applied a series of boronate affinity monolithic columns for the selective enrichment of nucleosides from human urine samples. The extracted samples were analyzed by micellar electrokinetic chromatography (MEKC) with UV detection. As the performance of the boronate affinity monolithic columns was gradually improved, the number of extracted components was increasing. Totally 11, 13, 13, 19 and 20 components were enriched from the urine samples by using Wulff-type boronate-functionalized monolithic column,<sup>41</sup> improved Wulff-type boronate-functionalized monolithic column,<sup>46</sup> AAPBA-silica hybrid monolithic column,<sup>47</sup> DFFPBA-functionalized monolithic column<sup>52</sup> and pyridinylboronic acid-functionalized organic-silica hybrid monolithic column,<sup>57</sup> respectively. Particularly, the pyridinylboronic acid-functionalized organic-silica hybrid monolithic column can be directly applied to urine samples without pH adjustment prior to the analysis due to its extremely low binding pH of 4.5 (the pH of human urine ranges from 4.5 to 8.0), which makes the monolith very promising for metabolomic analysis compared to the other monoliths. In addition, Xu and co-workers<sup>126</sup> developed an

line combination of BAC and reversed phase HPLC with UV detection. It allowed for determination of 11 urinary nucleosides by direct injection of urinary samples.

MS can provide structural information and has been a key analytical tool in metabolomic analysis. Kammerer and co-workers<sup>206</sup> established a coupling of HPLC with ESI ion-trap MS (ESI-IT MS) for the analysis of urinary nucleosides, based on pre-purification via boronate affinity chromatography followed by reversed phase chromatography. This method gave a LOD of between 0.1 and 9.6 pmol for 15 standard nucleosides. A urine sample of a breast cancer patient was investigated. Neutral loss of the ribose moiety (132 u) was used for the identification of urinary nucleosides. Totally 36 compounds were identified as nucleosides. In order to further elucidate structural identification of the metabolites from urine sample of tumour patients, they<sup>207</sup> also developed an approach for the identification of ribosylated metabolites in the 24-h urine of tumour patients suffering from lung, rectal, or head and neck cancer. The boronate affinity chromatography was used to isolate *cis*-diol-containing metabolites. The extracted metabolites were analyzed by the combination of accurate mass determination via Fourier transform ion cyclotron resonance MS (FTICR MS) and characteristic fragmentation patterns, produced by IT MS. In all, 22 metabolites derived from cellular RNA metabolism and related metabolic pathways were identified. In these identified compounds, four modified nucleosides were newly observed, including 2-methylthio-*N*<sup>6</sup>-(*cis*-hydroxyisopentenyl)-adenosine, 5-methoxycarbonylmethyl-2-thiouridine, *N*<sup>6</sup>-methyl-*N*<sup>6</sup>-threonyl carbamoyladenosine, and 2-methylthio-*N*<sup>6</sup>-threonylcarbamoyladenosine. However, the identified amount of ribosylated metabolites is not ideal enough due to the use of conventional boronate affinity media. To this end, the high-capacity and high-selectivity Fe<sub>3</sub>O<sub>4</sub>@SiO<sub>2</sub>@PEI-FPBA developed by Xu and co-workers<sup>78</sup> seemed advantageous, which allowed for the efficient extraction of nucleosides and ribosylated metabolites from human urine. The treated urine samples were analyzed by LC coupled with high-resolution MS. A total of 60 ion-pairs of ribose conjugates were obtained from urine after enrichment. Among them, 43 were identified to be nucleosides and other ribosylated metabolites. In these identified compounds, 9 low abundance modified nucleosides such as, 5-methylaminomethyl-2-thiouridine, urate-3-ribonucleoside, isoguanosine, 5-methoxy carbonylmethyluridine, 4-demethylwyosine and so on were found for the first time. In addition, 39 nucleosides were enriched and identified in a single analysis. This material can find more promising applications in the area of metabolomics to diagnose cancer and discover new cancer-related biomarkers. However, pH adjustment of urine sample was required, which may result in degradation of labile compounds.

The above mentioned combination was off-line mode. As such a mode is time-consuming in analysis, difficult to automate and reproduce, susceptible to sample loss and contamination of artefacts, it is not ideal for the high throughput analysis of urinary nucleoside and other ribosylated metabolites. To solve these issues, on-line combination mode is a more efficient alternative. Dudley and co-workers<sup>208</sup> established an on-line platform combining aprotic boronic acid chromatography (ApBAC)-based nucleoside trapping with an automated HPLC-MS system. Boronate affinity resin (Affi-Gel 601) was used as the extracting sorbent. Hydrophilic interaction chromatography (HILIC) was

used for the separation while ESI MS was used for the detection. As the loading and trapping of urinary nucleoside in ApBAC only occurred under aprotic conditions (100% acetonitrile), it was likely that a certain amount of acetonitrile can be transferred to the analytical HILIC column when switching the valves and mobile phases, which is particularly favourable for further separation of HILIC and identification of MS. The presence of 10 ribonucleosides and 11 modified ribonucleosides were confirmed from human urine. However, the selectivity of ApBAC toward *cis*-diol moieties is lost under aprotic environment, which greatly limits its further applications. To this end, an on-line solid-phase microextraction (SPME)-LC-MS/MS method was developed to comprehensively profile nucleosides and ribosylated metabolites in human urine (Fig. 14).<sup>209</sup> An AAPBA-silica hybrid monolithic capillary was used as the on-line SPME column, which exhibited good selectivity, low binding pH and high affinity toward nucleosides and ribosylated metabolites in human urine owing to the combination of AAPBA and “thiol-ene” click reaction. In this work, a pooled sample that included urines from 10 lung cancer patients, 10 colorectal cancer patients, 10 nasopharyngeal cancer patients or 10 healthy controls was used. 45 nucleosides and ribosylated metabolites were successfully identified and determined quantitatively in all the 4 types of human urine. Among these identified *cis*-diol-containing compounds, 5 modified nucleosides and ribosylated metabolites were first confirmed in human urine, including 3-hydroxychavicol 1-glucoside, 5-carbamoylmethyluridine, 6-hydroxyl-1,6-dihydropurine ribonucleoside, 1-ribosyl-*N*-acetylhistamine and 4-((1H-imidazol-2-yl)methyl)phenol-1-glucoside. Furthermore, the contents of 4 *cis*-diol-containing compounds, 5'-deoxy-5'-methylthioadenosine, *N*<sup>4</sup>-acetylcytidine, 1-ribosyl-*N*-propionyl histamine and *N*<sup>2</sup>,*N*<sup>2</sup>,7-trimethylguanosine increased more than 1.5 folds in all the 3 types of investigated cancers (lung cancer, colorectal cancer, and nasopharyngeal cancer) compared to healthy controls. These compounds may be used as potential indicators for the screening of cancers.

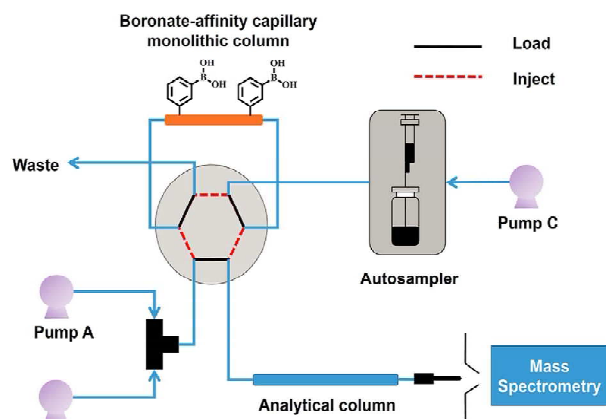


Fig. 14 Schematic illustration of the on-line SPME-LC-MS/MS system. Reproduced from ref. 209 with permission from Nature Publishing Group.

As compared with metabolic profiling in blood and urine, cell culture supernatants-based metabolomics can provide the great advantage of the exclusion of subsequent interferences along the excretion pathway, e.g. enzymatic actions in the blood stream, liver and kidney as well as the falsification by bacterial metabolites. Thus, cell culture supernatants-based metabolomics can generate unaltered metabolite patterns of cellular origin. In order to better understand the impaired RNA metabolism in breast cancer cells, Kammerer and co-workers<sup>210</sup> developed an

on-line 2D-chromatographic technique to examine these metabolites in the cell culture supernatants of the breast cancer cell line MCF-7. Nucleosides were isolated by boronate affinity gel (the first dimension) and subsequently analyzed by LC-IT MS.

In total, 36 metabolites were identified. Among the identified compounds, 26 modified ribonucleosides were included. Through the comparison of breast cancer cell line MCF-7 with mammary epithelial cells MCF-10A, 13 of the identified 26 modified ribonucleosides were increased in the cell culture supernatants of MCF-7 cells, with 5-methyluridine,  $N^2,N^2,7$ -trimethylguanosine,  $N^6$ -methyl- $N^6$ -threonylcarbamoyl-adenosine and 3-(3-aminocarboxypropyl)-uridine exhibiting the most significant differences. In addition, 1-ribosyl-4-carboxamido-5-aminoimidazole and *S*-adenosylmethionine were found only in the supernatants of MCF-7 cells. Clearly, the obtained results lead to new perspectives for modified nucleosides and related metabolites as possible markers for breast carcinoma *in vivo*.

### 3.4. Disease diagnostics

With the great developments of proteomics and metabolomics, a lot of compounds in real samples can be discovered as disease biomarkers. Especially, the glycosylation of proteins is associated with the occurrence of diverse diseases and many glycoproteins have been employed as disease biomarkers for clinical diagnosis.<sup>193,194</sup> Boronate affinity materials can be used as efficient binding tools to determine quantitatively disease biomarkers.

AFP and CEA have been routinely used as a biomarker in clinical screening for liver cancer.<sup>211,212</sup> A reliable and sensitive detection approach for AFP or CEA is of great importance in practical applications. Liu and co-workers<sup>213</sup> established an immunoassay for determination of AFP by using a boronate sepharose gel column as the antigen AFP collector in combination with flow injection chemiluminescence. First, the analyte AFP and excess HRP-anti-AFP was incubated. After that, free HRP-anti-AFP in the above mixture was captured by the immobilized AFP on the boronate affinity column. Then, the trapped HRP-anti-AFP was detected by flow injection chemiluminescence based on the reaction of luminol and hydrogen peroxide. Clearly, the AFP concentration in serum could be obtained via the indirect method. Changes of chemiluminescence responding to AFP concentrations were measured and the intensity decreased linearly when the AFP concentration was in the ranges of 5-120 and 300-1000 ng/mL, respectively ( $R = 0.9987$  and  $0.9998$ , respectively). The concentrations of five clinical serum AFP samples were determined to be 118.3, 335.9, 835.9, 335.9 and 44.7 ng/mL, respectively, which were in good agreement with those obtained by commercial electrochemiluminescent method. Shortly thereafter, a similar immunoassay for the determination of CEA was developed by Yang and co-workers.<sup>214</sup> The approach was based on the combination of a column packed with APBA-coated glass microbeads (as the antigen collector) and flow injection chemiluminescence. By using this approach, the chemiluminescence intensity decreased linearly with the increasing CEA concentration within the range of 3-30 ng/mL ( $R = 0.9980$ ). The concentrations of five serum CEA samples were evaluated to be 31.9, 83.3, 3.7, 5.9 and 223.6 ng/mL, respectively. These results are comparable to a commercial method.

Although the above mentioned approaches could be used for the detection of the serum AFP and CEA level in clinical diagnosis, the indirect competitive immunoreaction needs complex manipulation. Also, the relatively low affinity and poor selectivity of the above used boronate affinity materials toward targets were not able to guarantee the feasibility of these methods

in early clinical diagnosis. To solve these issues, an AFP-imprinted MIP array was used to replace the primary antibody in conventional ELISA.<sup>104</sup> Combined with chemiluminescence detection, the MIP array-based ELISA allowed for the specific detection of trace AFP in serum samples. The boronate affinity MIP array provided the specificity toward AFP while chemiluminescence detection ensured the detection sensitivity. Human serum samples spiked with different concentrations of AFP were determined. The LOD reached 1 ng/mL, which well meets the requirement for early clinical diagnosis. In this approach, secondary antibody and enzyme HRP were still inevitable. By replacing the secondary antibody and HRP with boronic acid-functionalized silver nanoparticles as the surface-enhanced Raman scattering (SERS) probes, Liu and co-workers<sup>215</sup> built up a unique antibody-free and enzyme-free ELISA called boronate affinity sandwich assay (BASA). BASA relied on the formation of sandwiches between boronate affinity MIPs, target glycoproteins and boronate affinity SERS probes (Fig. 15A). The MIP ensured the specificity while the SERS detection provided the sensitivity. As compared with fluorescence and chemiluminescence detection, SERS exhibited several significant advantages, such as ultrahigh sensitivity, less susceptibility to sample environment and possibility for on-site or field detection. With such significant advantages, BASA was successfully used for trace AFP detection in human serum. As shown in Fig. 15B, the intensity of the SERS signal was proportional to the logarithm of the AFP concentration within the range 1 to 10  $\mu\text{g/mL}$ . By using the standard addition method, the AFP concentration in a healthy serum sample was determined to be  $13.8 \pm 3.3$  ng/mL (Fig. 15C), which was in good agreement with the value by radioimmunoassay (10 ng/mL). BASA exhibited several significant advantages over conventional immunoassay, including low cost, high stability and fast speed. Clearly, BASA can be a promising approach for the detection of glycoprotein disease biomarkers in clinical diagnosis.

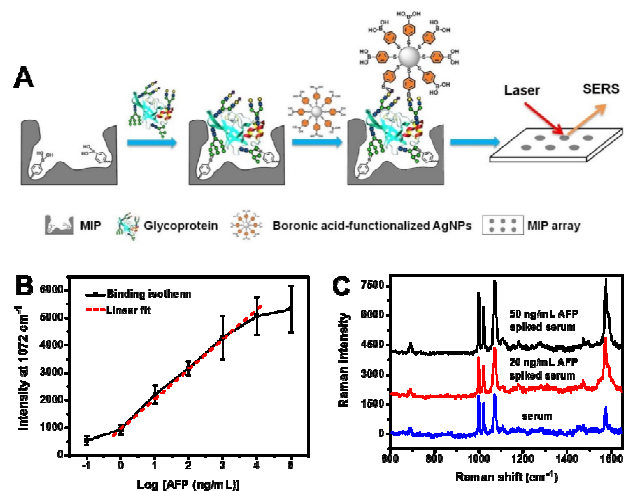


**Fig. 15** Schematic of the boronate affinity sandwich assay of glycoproteins (A), dependence of the intensity of the SERS signal on the concentration of the AFP solution (containing 100 mM phosphate buffer, pH 7.4) (B) and SERS spectra for serum samples spiked with different AFP concentrations (C). Adapted from ref. 215 with permission from John Wiley and Sons.

96-well microplate-based ELISA is a major platform for high throughput analysis of disease biomarkers. MIPs coated boronate affinity 96-well microplates have been used as efficient substitutes of antibody-coated microplates to develop a MIP-



based ELISA method.<sup>110,111</sup> In an AFP-imprinted MIP based ELISA, UV-vis absorbance detection with 3,3',5,5'-tetramethylbenzidine (TMB) staining of HRP was used to provide the sensitive detection of AFP.<sup>110</sup> Changes of absorbance responding to AFP concentrations were measured and it showed a good linearity within the range of 0-50 ng/mL ( $R^2 = 0.93$ ). The AFP concentration in a human serum was evaluated to be  $12 \pm 2.0$  ng/mL using the standard addition method, which was in good agreement with the above mentioned result ( $13.8 \pm 3.3$  ng/mL).<sup>215</sup> Unfortunately, secondary antibody and enzyme HRP were still required. Moreover, enzyme activity assay is also an important tool in clinical diagnostics. ALP, a glycoprotein enzyme that has been routinely used as an indicator for several diseases in clinical tests, was taken as a representative target enzyme. An ALP-imprinted MIP was directly used for activity assay since boronate affinity MIP could well retain the enzymatic activity of glycoprotein enzymes. The absorbance or the activity of ALP was proportional to ALP concentration within the range of 0-50 U/L ( $R^2 = 0.99$ ). According to the standard addition method, the ALP concentration in a human serum was evaluated to be  $482 \pm 58$  U/L, which was a little lower than the value by the IFCC (International Federation of Clinical Chemistry and Laboratory Medicine) standard method (537 U/L).<sup>216</sup> The difference between these results is attributed to the absence of the sample matrix in the final sample solution for signal readout in this applied method. The removal of the sample matrix could eliminate the interference of the sample matrix with the optical detection. Thus, the result may be more reliable. As a lot of important enzymes are glycoproteins and the boronate affinity molecular imprinting method is generally applicable for glycoproteins, the proposed method exhibits a promising prospect in real-world applications.

### 3.5. Aptamer selection

Aptamers are single-stranded DNA (ssDNA) or RNA oligonucleotides capable of binding specifically certain targets.<sup>217,218</sup> The high affinity and specificity make aptamers attractive alternatives to antibodies. Highly efficient aptamer selection is indispensable prior to use. Nucleic acid aptamers are usually selected from a large random oligonucleic acid library by systematic evolution of ligands by exponential enrichment (SELEX).<sup>217,218</sup> It is a critical step to isolate target-binding ssDNA from the random pool in SELEX. As boronate affinity materials can bind *cis*-diol-containing biomolecules, such as glycoproteins, in a pH-mediated fashion, boronate affinity materials can be effective platforms for aptamer selection. Liu and co-workers<sup>219</sup> developed a boronate affinity monolithic capillary-based SELEX approach for efficient selection of glycoprotein-binding DNA aptamers owing to the significant advantages of monolithic capillary and boronate affinity. The key to this approach is the facile immobilization of target glycoprotein and easy recovery of bound species just simply switching the pH condition, avoiding tedious procedure and harsh conditions. The principle of the approach is presented in Fig. 16A. A 3-carboxybenzoboroxole-functionalized monolithic capillary<sup>49</sup> was used as the selection platform due to its excellent selectivity and high affinity toward glycoproteins at physiological pH condition. A target glycoprotein dissolved in a protein loading buffer was first continuously pumped into the boronate affinity monolithic capillary until all the boronic acid moieties on the monolith were saturated by the target. Unbound target glycoprotein was washed away by the protein loading buffer. Then the monolithic capillary was equilibrated with a DNA loading buffer. After that, a random ssDNA library was pumped to the monolithic capillary and incubated with the immobilized

target at room temperature for a certain period. Unbound ssDNA species were removed by rinsing the capillary with the DNA loading buffer. Bound species were eluted along with the target by an acetic elution solution and consecutively collected. After evaluation with CE, desired fractions were combined and used for PCR amplification. The amplified species were submitted for a new round of selection, and the process was repeated again and again until the binding affinity met the requirement or would not increase any more. Because of the employment of boronate affinity monolithic capillary, the approach overcame the major drawbacks existed in conventional SELEX methods. As depicted in Fig. 16B, the proposed SELEX endowed with rapid selection efficiency (only 6 rounds of selection or 2 days were needed), high specificity toward the target molecules, and minute reagent consumption. This approach may open up new avenues to the rapid and efficient aptamer selection using boronate affinity materials.

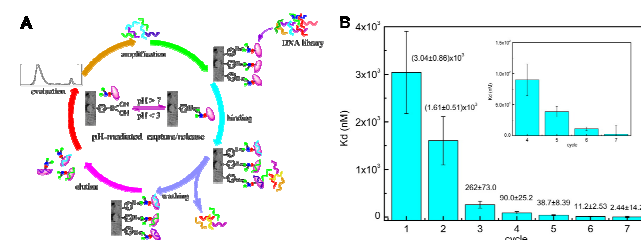


**Fig. 16** Schematic illustration of the boronate affinity monolithic capillary-based SELEX approach (A) and bulk  $K_d$  values for the ssDNA selected at each cycle (B). Adapted from ref. 219 with permission from American Chemical Society.

## 4. Conclusions and perspectives

Boronate affinity materials have attracted increasing attention in recent years. A variety of boronate affinity materials with different ligand structure and material structure have been successfully prepared, including macroporous monoliths, mesoporous materials, nanoparticles, molecularly imprinted polymers and temperature-responsive materials. Due to the efforts of reducing the binding pH and increasing the selectivity by adjusting ligand structure, the usefulness of boronate affinity materials to real samples has been greatly improved. On the other hand, multivalent synergistic effect has proved to be an effective strategy to enhance the binding strength toward glycoproteins, boronate avidity materials have allowed for the selective enrichment of glycoproteins of trace concentration. Furthermore, combination of the affinity of boronic acid with the properties of the material structure provided new features for affinity recognition and separation. A protein A mimic material has been available through combining the chemical affinity and selectivity of boronic acids with the size selectivity of nanopores of macroporous monoliths. In a similar sense, through combining the chemical affinity and selectivity of boronic acids with the size and shape selectivity of nanoscale imprinted cavities, boronate affinity MIPs exhibited highly favourable features, including wider binding pH, high affinity, high specificity and superb tolerance for interference. Owing to these significant advances, boronate affinity materials have found important applications in affinity separation, proteomics, metabolomics, disease diagnostics and aptamer selection. As to future development, we believe combination of boronate affinity materials with other desirable properties such as signal reporting will be an important direction. We foresee that boronate affinity materials will find more and more promising applications in separation and

molecular recognition in the future.

## Acknowledgements

We acknowledge the financial support of the National Science Fund for Distinguished Young Scholars (No. 21425520) and the general grant (No. 21275073) from the National Natural Science Foundation of China as well as the Key Grant of 973 Program (No. 2013CB911202) from the Ministry of Science and Technology of China.

## Notes and references

State Key Laboratory of Analytical Chemistry for Life Science and Collaborative Innovation Center of Chemistry for Life Sciences, School of Chemistry and Chemical Engineering, Nanjing University, 22 Hankou Road, Nanjing 210093 (China). Fax: (+86) 25-8368-5639 E-mail: zhenliu@nju.edu.cn.

† Electronic Supplementary Information (ESI) available: [details of any supplementary information available should be included here]. See DOI: 10.1039/b000000x/

‡ Footnotes should appear here. These might include comments relevant to but not central to the matter under discussion, limited experimental and spectral data, and crystallographic data.

- 1 X. C. Liu and W. H. Scouten, *Methods Mol. Biol.*, 2000, **147**, 119-128.
- 2 H. Y. Li and Z. Liu, *Trends Anal. Chem.*, 2012, **37**, 148-161.
- 3 R. Nishiyabu, Y. Kubo, T. D. James and J. S. Fossey, *Chem. Commun.*, 2011, **47**, 1106-1123.
- 4 J.-B. Biot, *Mem. Acad. Sci.*, 1838, **16**, 229-396.
- 5 F. K. Bell, C. J. Carr, W. E. Evans and J. C. Krantz, *J. Phy. Chem.*, 1937, **42**, 507-513.
- 6 J. Boeseken, *Adv. Carbohydr. Chem.*, 1949, **4**, 189-210.
- 7 A. B. Foster, *Adv. Carbohydr. Chem.*, 1957, **12**, 81-115.
- 8 J. M. Sugihara and C. M. Bowman, *J. Am. Chem. Soc.*, 1958, **80**, 2443-2446.
- 9 E. J. Bourne, E. M. Lees and H. Weigel, *J. Chromatogr.*, 1963, **11**, 253-257.
- 10 H. L. Weith, J. L. Wiebers and P. T. Gilham, *Biochem.*, 1970, **9**, 4396-4401.
- 11 A. M. Yurkevich, E. A. Ivanova and E. I. Pichuzhkina, *Carbohydr. Res.*, 1975, **43**, 215-224.
- 12 V. K. Akparov and V. M. Stepanov, *J. Chromatogr.*, 1978, **155**, 329-336.
- 13 M. Glad, S. Ohlson, L. Hansson, M. O. Mansson and K. Mosbach, *J. Chromatogr. A*, 1980, **200**, 254-260.
- 14 T. A. Myohanen, V. Bouriotis and P. D. G. Dean, *Biochem. J.*, 1981, **197**, 683-688.
- 15 B. J. B. Johnson, *Biochem.*, 1981, **20**, 6103-6108.
- 16 A. K. Mallia, G. T. Hermanson, R. I. Krohn, E. K. Fujimoto and P. K. Smith, *Anal. Lett.*, 1981, **14**, 649-661.
- 17 D. C. Klenk, G. T. Hermanson, R. I. Krohn, E. K. Fujimoto, A. Krishna Mallia, P. K. Smith, J. D. England, H. M. Wiedmeyer, R. R. Little and D. E. Goldstein, *Clin. Chem.*, 1982, **28**, 2088-2094.
- 18 G. Wulff, *Pure. Appl. Chem.*, 1982, **54**, 2093-2102.
- 19 G. T. Williams, A. P. Johnstone and P. D. G. Dean, *Biochem. J.*, 1982, **205**, 167-171.
- 20 A. Bergold and W. H. Scouten, *Borate chromatography, in Solid Phase Biochemistry*, (Scouten, W. H., ed.), Wiley, New York, 1983, 149-187.
- 21 F. A. Middle, A. J. Bellingham and P. D. G. Dean, *Biochem. J.*, 1983, **209**, 771-779.
- 22 R. Flückiger, T. Woodtli and W. Berger, *Diabetes*, 1984, **33**, 73-76.
- 23 C. J. Hawkins, M. F. Lavin, D. L. Parry and I. L. Ross, *Anal. Biochem.*, 1986, **159**, 187-190.
- 24 T. Yamamoto, Y. Amuro, Y. Matsuda, H. Nakaok, S. Shimomura, T. Hata and K. Higashino, *J. Gastroenterol.*, 1991, **86**, 495-499.
- 25 E. Bisse and H. Wieland, *J. Chromatogr. B.*, 1992, **575**, 223-228.
- 26 X. C. Liu and W. H. Scouten, *J. Mol. Recognit.*, 1996, **9**, 462-467.
- 27 T. Koyama and K. Terauchi, *J. Chromatogr. B*, 1996, **679**, 31-40.
- 28 F. Frantzen, K. Grimsrud, D. E. Heggli and E. Sundrehagen, *Clin. Chim. Acta*, 1997, **263**, 207-224.
- 29 N. Singhl and R. C. Willson, *J. Chromatogr. A*, 1999, **840**, 205-213.
- 30 S. Senel, S. T. C. Amli, M. Tuncel and A. Tuncel, *J. Chromatogr. B*, 2002, **769**, 283-295.
- 31 R. R. Little, H. Vesper, C. L. Rohlfing, M. Ospina, S. Safar-Pour and W. L. Roberts, *Clin. Chem.*, 2005, **51**, 264-265.
- 32 E. A. Lowe, M. Lu, A. Wang, H. Cortez, D. Ellis and X. C. Liu, *J. Sep. Sci.*, 2006, **29**, 959-965.
- 33 O. G. Potter, M. C. Breadmore and E. F. Hilder, *Analyst*, 2006, **131**, 1094-1096.
- 34 M. Chen, Y. Lu, Q. Ma, L. Guo and Y. Q. Feng, *Analyst*, 2009, **134**, 2158-2164.
- 35 L. B. Ren, Z. Liu, M. M. Dong, M. L. Ye and H. F. Zou, *J. Chromatogr. A*, 2009, **1216**, 4768-4774.
- 36 L. B. Ren, Y. C. Liu, M. M. Dong and Z. Liu, *J. Chromatogr. A*, 2009, **1216**, 8421-8435.
- 37 L. B. Ren, Z. Liu, Y. C. Liu, P. Dou and H. Y. Chen, *Angew. Chem. Int. Ed.*, 2009, **48**, 6704-6707.
- 38 X. L. Sun, R. Liu, X. W. He, L. X. Chen and Y. K. Zhang, *Talanta*, 2010, **81**, 856-864.
- 39 Y. C. Liu, L. B. Ren and Z. Liu, *Chem. Commun.*, 2011, **47**, 5067-5069.
- 40 F. Yang, Z. A. Lin, X. W. He, L. X. Chen and Y. K. Zhang, *J. Chromatogr. A*, 2011, **1218**, 9194-9201.
- 41 H. Y. Li, Y. C. Liu, J. Liu and Z. Liu, *Chem. Commun.*, 2011, **47**, 8169-8172.
- 42 Z. A. Lin, J. L. Pang, Y. Lin, H. Huang, Z. W. Cai, L. Zhang and G. N. Chen, *Analyst*, 2011, **136**, 3281-3288.
- 43 Z. A. Lin, J. L. Pang, H. H. Yang, Z. W. Cai, L. Zhang and G. N. Chen, *Chem. Commun.*, 2011, **47**, 9675-9677.
- 44 H. Huang, Z. A. Lin, Y. Lin, X. B. Sun, Y. Y. Xie, L. Zhang and G. N. Chen, *J. Chromatogr. A*, 2012, **1251**, 82-90.
- 45 Y. C. Liu, Y. Lu and Z. Liu, *Chem. Sci.*, 2012, **3**, 1467-1471.
- 46 H. Y. Li, H. Y. Wang, Y. C. Liu and Z. Liu, *Chem. Commun.*, 2012, **48**, 4115-4117.
- 47 Q. J. Li, C. C. Lü, H. Y. Li, Y. C. Liu, H. Y. Wang, X. Wang and Z. Liu, *J. Chromatogr. A*, 2012, **1256**, 114-120.
- 48 F. Yang, J. Mao, X. W. He, L. X. Chen and Y. K. Zhang, *Anal. Bioanal. Chem.*, 2013, **405**, 5321-5331.
- 49 F. Yang, J. Mao, X. W. He, L. X. Chen and Y. K. Zhang, *Anal. Bioanal. Chem.*, 2013, **405**, 6639-6648.
- 50 Y. Lu, Z. J. Bie, Y. C. Liu and Z. Liu, *Analyst*, 2013, **138**, 290-298.
- 51 S. T. Wang, D. Chen, J. Ding, B. F. Yuan and Y. Q. Feng, *Chem. Eur. J.*, 2013, **19**, 606-612.
- 52 Q. J. Li, C. C. Lü and Z. Liu, *J. Chromatogr. A*, 2013, **1305**, 123-130.

- 53 X. Wang, Y. C. Liu, L. B. Ren, H. Y. Li and Z. Liu, *Anal. Methods*, 2013, **5**, 5444-5449.
- 54 Q. Yang, D. H. Huang, S. X. Jin, H. Zhou and P. Zhou, *Analyst*, 2013, **138**, 4752-4755.
- 55 Z. A. Lin, H. Huang, S. H. Li, J. Wang, X. Q. Tan, L. Zhang and G. N. Chen, *J. Chromatogr. A*, 2013, **1271**, 115-123.
- 56 Z. J. Bie, Y. Chen, H. Y. Li, R. H. Wu and Z. Liu, *Anal. Chim. Acta*, 2014, **834**, 1-8.
- 57 D. J. Li, Q. J. Li, S. S. Wang, J. Ye, H. Y. Nie and Z. Liu, *J. Chromatogr. A*, 2014, **1339**, 103-109.
- 58 Q. Yang, D. H. Huang and P. Zhou, *Analyst*, 2014, **139**, 987-991.
- 59 C. Wu, Y. Liang, Q. Zhao, Y. Y. Qu, S. Zhang, Q. Wu, Z. Liang, L. H. Zhang and Y. K. Zhang, *Chem. Eur. J.*, 2014, **20**, 8737-8743.
- 60 D. J. Li, Y. Li, X. L. Li, Z. J. Bie, X. H. Pang, Q. Zhang and Z. Liu, *J. Chromatogr. A*, 2015, **1384**, 88-96.
- 61 Y. W. Xu, Z. X. Wu, L. J. Zhang, H. J. Lu, P. Y. Yang, P. A. Webley and D. Y. Zhao, *Anal. Chem.*, 2009, **81**, 503-508.
- 62 L. T. Liu, Y. Zhang, L. Zhang, G. Q. Yan, J. Yao, P. Y. Yang and H. J. Lu, *Anal. Chim. Acta*, 2012, **753**, 64-72.
- 63 J. Tan, H. F. Wang and X. P. Yan, *Anal. Chem.*, 2009, **81**, 5273-5280.
- 64 W. Zhou, N. Yao, G. P. Yao, C. H. Deng, X. M. Zhang and P. Y. Yang, *Chem. Commun.*, 2008, 5577-5579.
- 65 J. Tang, Y. C. Liu, D. W. Qi, G. P. Yao, C. H. Deng and X. M. Zhang, *Proteomics*, 2009, **9**, 5046-5055.
- 66 G. P. Yao, H. Y. Zhang, C. H. Deng, H. J. Lu, X. M. Zhang and P. Y. Yang, *Rapid Commun. Mass Spectrom.*, 2009, **23**, 3493-3500.
- 67 L. J. Zhang, Y. W. Xu, H. L. Yao, L. Q. Xie, J. Yao, H. J. Lu and P. Y. Yang, *Chem. Eur. J.*, 2009, **15**, 10158-10166.
- 68 J. Tang, Y. Liu, P. Yin, G. P. Yao, G. Q. Yan, C. H. Deng and X. M. Zhang, *Proteomics*, 2010, **10**, 2000-2014.
- 69 D. W. Qi, H. Y. Zhang, J. Tang, C. H. Deng and X. M. Zhang, *J. Phys. Chem. C*, 2010, **114**, 9221-9226.
- 70 W. W. Shen, C. N. Ma, S. F. Wang, H. M. Xiong, H. J. Lu and P. Y. Yang, *Chem. Asian J.*, 2010, **5**, 1185-1191.
- 71 T. A. Pham, N. A. Kumar and Y. T. Jeong, *Colloids Surf. A: Physicochem. Eng. Aspects*, 2010, **370**, 95-101.
- 72 Z. A. Lin, J. N. Zheng, F. L. Lin, L. Zhang, Z. W. Cai and G. N. Chen, *J. Mater. Chem.*, 2011, **21**, 518-524.
- 73 L. Liang and Z. Liu, *Chem. Commun.*, 2011, **47**, 2255-2257.
- 74 P. Dou and Z. Liu, *Anal. Bioanal. Chem.*, 2011, **399**, 3423-3429.
- 75 X. H. Zhang, X. W. He, L. X. Chen and Y. K. Zhang, *J. Mater. Chem.*, 2012, **22**, 16520-16526.
- 76 Y. Y. Qu, X. Liu, Z. Liang, L. H. Zhang and Y. K. Zhang, *Chem. Eur. J.*, 2012, **18**, 9056-9062.
- 77 Z. A. Lin, J. N. Zheng, Z. W. Xia, H. H. Yang, L. Zhang and G. N. Chen, *RSC Adv.*, 2012, **2**, 5062-5065.
- 78 H. Li, Y. H. Shan, L. Z. Qiao, A. Dou, X. Z. Shi and G. W. Xu, *Anal. Chem.*, 2013, **85**, 11585-11592.
- 79 G. B. Xu, W. Zhang, L. M. Wei, H. J. Lu and P. Y. Yang, *Analyst*, 2013, **138**, 1876-1885.
- 80 H. Y. Wang, Z. J. Bie, C. C. Lü and Z. Liu, *Chem. Sci.*, 2013, **4**, 4298-4303.
- 81 M. R. Pan, Y. F. Sun, J. Zheng and W. L. Yang, *ACS Appl. Mater. Interfaces*, 2013, **5**, 8351-8358.
- 82 M. B. Liu, L. J. Zhang, Y. W. Xu, P. Y. Yang and H. J. Lu, *Anal. Chim. Acta*, 2013, **788**, 129-134.
- 83 S. Zhang, X. W. He, L. X. Chen and Y. K. Zhang, *New J. Chem.*, 2014, **38**, 4212-4218.
- 84 X. H. Zhang, X. W. He, L. X. Chen and Y. K. Zhang, *J. Mater. Chem. B*, 2014, **2**, 3254-3262.
- 85 Y. L. Wang, M. B. Liu, L. Q. Xie, C. Y. Fang, H. M. Xiong and H. J. Lu, *Anal. Chem.*, 2014, **86**, 2057-2064.
- 86 J. X. Liu, Y. Y. Qu, K. G. Yang, Q. Wu, Y. C. Shan, L. H. Zhang, Z. Liang and Y. K. Zhang, *ACS Appl. Mater. Interfaces*, 2014, **6**, 2059-2066.
- 87 Z. F. Xu, K. M. A. Uddin, T. Kamra, J. Schnadt and L. Ye, *ACS Appl. Mater. Interfaces*, 2014, **6**, 1406-1414.
- 88 J. X. Liu, K. G. Yang, Y. Y. Qu, S. W. Li, Q. Wu, Z. Liang, L. H. Zhang and Y. K. Zhang, *Chem. Commun.*, 2015, **51**, 3896-3898.
- 89 G. Wulff, R. Grobe-Einsler, W. Vesper and A. Sarhan, *Makromol. Chem.*, 1977, **178**, 2817-2825.
- 90 G. Wulff, *Pure. Appl. Chem.*, 1982, **54**, 2093-2102.
- 91 G. Wulff and S. Schauhoff, *J. Org. Chem.*, 1991, **56**, 395-400.
- 92 J. Kugimiya, J. Matsui, T. Takeuchi, K. Yano, H. Muguruma, A. V. Elgersma and I. Karube, *Anal. Lett.*, 1995, **28**, 2317-2323.
- 93 A. Friggeri, H. Kobayashi, S. Shinkai and D. N. Reinhoudt, *Angew. Chem. Int. Ed.*, 2001, **40**, 4729-4731.
- 94 N. Sallacan, M. Zayats, T. Bourenko, A. B. Kharitonov and I. Willner, *Anal. Chem.*, 2002, **74**, 702-712.
- 95 T. Takeuchi, N. Murase, H. Maki, T. Mukawa and H. Shinmori, *Org. Biomol. Chem.*, 2006, **4**, 565-568.
- 96 F. Bretona, R. Delépée, D. Jégourel, D. Deville-Bonneb and L. A. Agrofoglio, *Anal. Chim. Acta*, 2008, **616**, 222-229.
- 97 Y. Ben-Amram, M. Riskin and I. Willner, *Analyst*, 2010, **135**, 2952-2959.
- 98 B. Okutucu and S. Önal, *Talanta*, 2011, **87**, 74-79.
- 99 N. Henry, R. Delépée, J. M. Seigneuret and L. A. Agrofoglio, *Talanta*, 2012, **99**, 816-823.
- 100 T. Huynh, A. Pietrzyk-Le, C. Bikram K.C., K. R. Noworyta, J. W. Sobczak, P. S. Sharma, F. D'Souza and W. Kutner, *Biosens. Bioelectron.*, 2013, **41**, 634-641.
- 101 L. Gu, X. Y. Jiang, Y. Liang, T. S. Zhou and G. Y. Shi, *Analyst*, 2013, **138**, 5461-5469.
- 102 W. L. Yang, S. M. Huang, Q. Z. Wu and J. F. He, *J. Polym. Res.*, 2014, **21**, 383-389.
- 103 M. Glad, O. Norrlov, B. Sellergren, N. Siegbahn and K. Mosbach, *J. Chromatogr. A*, 1985, **347**, 11-23.
- 104 L. Li, Y. Lu, Z. J. Bie, H. Y. Chen and Z. Liu, *Angew. Chem. Int. Ed.*, 2013, **52**, 7451-7454.
- 105 Y. X. Li, M. Hong, M. Miao, Q. Bin, Z. Y. Lin, Z. W. Cai and G. N. Chen, *J. Mater. Chem. B*, 2013, **1**, 1044-1051.
- 106 F. X. Gao, X. T. Ma, X. W. He, W. Y. Li and Y. K. Zhang, *Colloids Surf. A: Physicochem. Eng. Aspects*, 2013, **433**, 191-199.
- 107 Z. A. Lin, J. Wang, X. Q. Tan, L. X. Sun, R. F. Yu, H. H. Yang and G. N. Chen, *J. Chromatogr. A*, 2013, **1319**, 141-147.
- 108 W. Zhang, W. Liu, P. Li, H. B. Xiao, H. Wang and B. Tang, *Angew. Chem. Int. Ed.*, 2014, **53**, 12489-12493.
- 109 S. S. Wang, J. Ye, Z. J. Bie and Z. Liu, *Chem. Sci.*, 2014, **5**, 1135-1140.
- 110 X. D. Bi and Z. Liu, *Anal. Chem.*, 2014, **86**, 959-966.
- 111 X. D. Bi and Z. Liu, *Anal. Chem.*, 2014, **86**, 12382-12389.
- 112 Z. A. Lin, L. X. Sun, W. Liu, Z. W. Xia, H. H. Yang and G. N. Chen, *J. Mater. Chem. B*, 2014, **2**, 637-643.
- 113 E. Uğuzdoğan, H. Kayı, E. B. Denkbaş, S. Patır and A. Tuncel, *Polym. Int.*, 2003, **52**, 649-657.
- 114 B. Elmas, M. A. Onur, S. Şenel and A. Tuncel, *Colloids Surf. A: Physicochem. Eng. Aspects*, 2004, **232**, 253-259.
- 115 B. Elmas, S. Senel and A. Tuncel, *React. Funct. Polym.*, 2007, **67**, 87-96.
- 116 G. Carré de Lusançay, S. Norvez and I. Iliopoulos, *Eur. Polym. J.*, 2010, **46**, 1367-1373.

- 117 Q. Jin, L. P. Lv, G. Y. Liu, J. P. Xu and J. Ji, *Polymer*, 2010, **51**, 3068-3074.
- 118 Z. J. Liu, K. Ullah, L. P. Su, F. Lv, Y. L. Deng, R. J. Dai, Y. J. Li and Y. K. Zhang, *J. Mater. Chem.*, 2012, **22**, 18753-18756.
- 119 Z. F. Xu, K. Mohammad Ahsan Uddin and L. Ye, *Macromolecules*, 2012, **45**, 6464-6470.
- 120 Y. Man, G. Peng, X. F. Lv, Y. L. Liang, Y. Wang, Y. Chen and Y. L. Deng, *Chromatographia*, 2015, **78**, 157-162.
- 121 Y. Man, G. Peng, J. S. Wang and Y. L. Deng, *J. Sep. Sci.*, 2015, **38**, 339-345.
- 122 Q. J. Li, X. Y. Tu, J. Ye, Z. J. Bie, X. D. Bi and Z. Liu, *Chem. Sci.*, 2014, **5**, 4065-4069.
- 123 J. N. Cambre and B. S. Sumerlin, *Polymer*, 2011, **52**, 4631-4643.
- 124 Y. Guan and Y. J. Zhang, *Chem. Soc. Rev.*, 2013, **42**, 8106-8121.
- 125 X. Li, J. Pennington, J. F. Stobaugh and C. Schoeich, *Anal. Biochem.*, 2008, **372**, 227-236.
- 126 F. L. Li, X. J. Zhao and G. W. Xu, *Chin. J. Anal. Chem.*, 2006, **34**, 1366-1370.
- 127 A. Matsumoto, K. Yamamoto, R. Yoshida, K. Kataoka, T. Aoyagi and Y. Miyahara, *Chem. Commun.*, 2010, **46**, 2203-2205.
- 128 G. Wulff, M. Lauer and H. Bohnke, *Angew. Chem. Int. Ed. Engl.*, 1984, **23**, 741-742.
- 129 M. Berube, M. Dowlut and D. G. Hall, *J. Org. Chem.*, 2008, **73**, 6471-6479.
- 130 M. Dowlut and D. G. Hall, *J. Am. Chem. Soc.*, 2006, **128**, 4226-4227.
- 131 A. Pal, M. Berube and D. G. Hall, *Angew. Chem. Int. Ed.*, 2010, **49**, 1492-1495.
- 132 L. K. Mohler and A. W. Czarnik, *J. Am. Chem. Soc.*, 1993, **115**, 2998-2999.
- 133 F. C. Fischer and E. Havinga, *Red. Trao. Chim. Pays.-Bas.*, 1974, **93**, 21-24.
- 134 K. T. Kim, J. J. LM. Cornelissen, R. J. M. Nolte and J. C. M. van Hest, *J. Am. Chem. Soc.*, 2009, **131**, 13908-13909.
- 135 T. D. James, K. R. A. S. Sandanayake and S. Shinkai, *Nature*, 1995, **374**, 345-347.
- 136 C. C. Lü, H. Y. Li, H. Y. Wang and Z. Liu, *Anal. Chem.*, 2013, **85**, 2361-2369.
- 137 J. Yan, G. Springsteen, S. Deeter and B. H. Wang, *Tetrahedron*, 2004, **60**, 11205-11209.
- 138 H. Otsuka, E. Uchimura, H. Koshino, T. Okano and K. Kataoka, *J. Am. Chem. Soc.*, 2003, **125**, 3493-3502.
- 139 X. C. Liu, *Chin. J. Chromatogr.*, 2006, **24**, 73-80.
- 140 M. Mammen, S. K. Choi and G. M. Whitesides, *Angew. Chem. Int. Ed.*, 1998, **37**, 2754-2794.
- 141 G. M. Pavan, A. Danani, S. Priel and D. K. Smith, *J. Am. Chem. Soc.*, 2009, **131**, 9686-9694.
- 142 J. M. J. Fréchet, *Science*, 1994, **263**, 1710-1715.
- 143 D. A. Tomalia, A. M. Naylor and W. A. Goddard, *Angew. Chem., Int. Ed. Engl.*, 1990, **29**, 138-175.
- 144 S. Hjerten, Y. M. Li, J. L. Liao, J. Mohammad, K. Nakazato and G. Pettersson, *Nature*, 1992, **356**, 810-811.
- 145 F. Svec and J. M. Fréchet, *Science*, 1996, **273**, 205-211.
- 146 N. Tsujioka, N. Hira, S. Aoki, N. Tanaka and K. Hosoya, *Macromolecules*, 2005, **38**, 9901-9903.
- 147 C. P. Desilets, M. A. Rounds and F. E. Regnier, *J. Chromatogr. A*, 1991, **544**, 25-29.
- 148 R. J. Tian, H. Zhang, M. L. Ye, X. G. Jiang, L. H. Hu, X. Li, X. H. Bao and H. F. Zou, *Angew. Chem. Int. Ed.*, 2007, **46**, 962-965.
- 149 R. J. Tian, L. B. Ren, H. J. Ma, X. Li, L. H. Hu, M. L. Ye, R. A. Wu, Z. J. Tian, Z. Liu and H. F. Zou, *J. Chromatogr. A*, 2009, **1216**, 1270-1278.
- 150 H. C. Kolb, M. G. Finn and K. B. Sharpless, *Angew. Chem. Int. Ed.*, 2001, **40**, 2004-2021.
- 151 J. E. Moses and A. D. Moorhouse, *Chem. Soc. Rev.*, 2007, **36**, 1249-1262.
- 152 J. S. Beck, J. C. Vartuli, W. J. Roth, M. E. Leonowicz, C. T. Kresge, K. D. Schmitt, C. T. W. Chu, D. H. Olson and E. W. Sheppard, *J. Am. Chem. Soc.*, 1992, **114**, 10834-10843.
- 153 D. Y. Zhao, J. L. Feng, Q. S. Huo, N. Melosh, G. H. Fredrickson, B. F. Chmelka and G. D. Stucky, *Science*, 1998, **279**, 548-552.
- 154 Y. Meng, D. Gu, F. Q. Zhang, Y. F. Shi, L. Cheng, D. Feng, Z. X. Wu, Z. X. Chen, Y. Wan, A. Stein and D. Y. Zhao, *Chem. Mater.*, 2006, **18**, 4447-4464.
- 155 G. Elizabeth, *Trends Anal. Chem.*, 2012, **46**, 1-14.
- 156 L. S. Ana, M. O. Riansares, S. L. Jon and C. Carmen, *Anal. Methods*, 2014, **6**, 38-56.
- 157 D. Sykora, V. Kasicka, I. Miksik, P. Rezanka, K. Zaruba, P. Matejka and V. Krai, *J. Sep. Sci.*, 2010, **33**, 372-387.
- 158 V. Matsura, Y. Guari, J. Larionova, C. Guérin, A. Caneschi, C. Sangregorio, E. Lancelle-Beltran, A. Mehdi and R. J. P. Corriu, *J. Mater. Chem.*, 2004, **14**, 3026-3033.
- 159 S. C. Wuang, K. G. Neoh, E. T. Kang, D. W. Pack and D. E. Leckband, *J. Mater. Chem.*, 2007, **17**, 3354-3362.
- 160 Y. Liu, Y. Xue and J. Ji, *Mol. Cell. Proteomics*, 2007, **6**, 1428-1436.
- 161 P. R. Sudhir, H. F. Wu and Z. C. Zhou, *Anal. Chem.*, 2005, **77**, 7380-7385.
- 162 C. H. Teng, K. C. Ho, Y. S. Lin and Y. C. Chen, *Anal. Chem.*, 2004, **76**, 4337-4342.
- 163 A. H. Lu, E. L. Salabas and F. Schüth, *Angew. Chem. Int. Ed.*, 2007, **46**, 1222-1244.
- 164 G. Wulff and A. Sarhan, *Angew. Chem.*, 1972, **84**, 364-364.
- 165 G. Vlatakis, L. I. Andersson, R. Müller and K. Mosbach, *Nature*, 1993, **361**, 645-647.
- 166 G. Wulff, *Angew. Chem., Int. Ed. Engl.*, 1995, **34**, 1812-1832.
- 167 H. Shi, W. B. Tsai, M. D. Garrison, S. Ferrari and B. D. Ratner, *Nature*, 1999, **398**, 593-597.
- 168 Y. Hoshino, H. Koide, T. Urakami, H. Kanazawa, T. Kodama, N. Oku and K. J. Shea, *J. Am. Chem. Soc.*, 2010, **132**, 6644-6645.
- 169 K. Mosbach, *Trends Biochem. Sci.*, 1994, **19**, 9-14.
- 170 M. Kempe, M. Glad and K. Mosbach, *J. Mol. Recognit.*, 1995, **8**, 35-39.
- 171 Y. Li, H. Yang, Q. You, Z. Zhuang and X. Wang, *Anal. Chem.*, 2006, **78**, 317-320.
- 172 N. Nishino, C. S. Huang and K. J. Shea, *Angew. Chem. Int. Ed.*, 2006, **45**, 2392-2396.
- 173 A. A. Özcan, R. Say, A. Denizli and A. Ersöz, *Anal. Chem.*, 2006, **78**, 7253-7258.
- 174 X. T. Shen and L. Ye, *Chem. Commun.*, 2011, **47**, 10359-10361.
- 175 L. Qin, X. W. He, W. Zhang, W. Y. Li and Y. K. Zhang, *Anal. Chem.*, 2009, **81**, 7206-7216.
- 176 A. Nematollahzadeh, W. Sun, C. S. A. Aureliano, D. Lütkemeyer, J. Stute, M. J. Abdekhodaie, A. Shojaei and B. Sellergren, *Angew. Chem., Int. Ed.*, 2011, **50**, 495-498.
- 177 L. Qin, X. He, W. Zhang, W. Li and Y. Zhang, *J. Chromatogr. A*, 2009, **1216**, 807-814.
- 178 Z. Lin, F. Yang, X. W. He, X. M. Zhao and Y. K. Zhang, *J. Chromatogr. A*, 2009, **1216**, 8612-8622.



- 179 H. Yang, S. Zhang, F. Tan, Z. Zhuang and X. Wang, *J. Am. Chem. Soc.*, 2005, **127**, 1378-1379.
- 180 A. Kumar, A. Srivastava, I. Y. Galaev and B. Mattiasson, *Prog. Polym. Sci.*, 2007, **32**, 1205-1237.
- 5 181 P. Maharjan, B. W. Woonton, L. E. Bennett, G. W. Smithers, K. DeSilva and M. T. W. Hearn, *Innovative Food Sci. Emerging Technol.*, 2008, **9**, 232-242.
- 182 D. Roy, J. N. Cambre and B. S. Sumerlin, *Prog. Polym. Sci.*, 2010, **35**, 278-301.
- 10 183 H. B. Du, R. Wickramasinghe and X. D. Qian, *J. Phys. Chem. B*, 2010, **114**, 16594-16604.
- 184 I. Shechter, O. Ramon, I. Portnaya, Y. Paz and Y. D. Livney, *Macromolecules*, 2010, **43**, 480-487.
- 185 J. Kost, T. A. Horbett, B. D. Ratner and M. Singh, *J. Biomed. Mater. Res.*, 1985, **19**, 1117-1133.
- 15 186 A. Matsumoto, S. Ikeda, A. Harada and K. Kataoka, *Biomacromolecules*, 2003, **4**, 1410-1416.
- 187 H. Dosch, *Appl. Surf. Sci.*, 2001, **182**, 192-195.
- 188 M. K. Kidder, P. F. Britt, Z. T. Zhang, S. Dai, E. W. Hagaman, A. L. Chaffee and A. C. Buchanan, *J. Am. Chem. Soc.*, 2005, **127**, 6353-6360.
- 20 189 M. V. Wolkin, J. Jorne, P. M. Fauchet, G. Allan and C. Delerue, *Phys. Rev. Lett.*, 1999, **82**, 197-200.
- 190 Y. Chen, S. S. Wang, J. Ye, D. J. Li, Z. Liu and X. C. Wu, *Nanoscale*, 2014, **6**, 9563-9567.
- 25 191 X. H. Pan, Y. Chen, P. X. Zhao, D. J. Li and Z. Liu, *Angew. Chem. Int. Ed.*, 2015, **54**, 6173-6176.
- 192 P. M. Rudd, T. Elliott, P. Cresswell, I. A. Wilson and R. A. Dwek, *Science*, 2001, **291**, 2370-2376.
- 30 193 J. A. Ludwig and J. N. Weinstein, *Nat. Rev. Cancer*, 2005, **5**, 845-856.
- 194 H. J. Gabius, *Biochem. Soc. Trans.*, 2011, **39**, 399-405.
- 195 H. Kaji, H. Saito, Y. Yamauchi, T. Shinkawa, M. Taoka, J. Hirabayashi, K. Kasai, N. Takahashi and T. Isobe, *Nat. Biotechnol.*, 2003, **21**, 667-672.
- 35 196 Z. B. Xu, X. W. Zhou, H. J. Lu, N. Wu, H. B. Zhao, L. N. Zhang, W. Zhang, Y. L. Liang, L. Y. Wang, Y. K. Liu, P. Y. Yang and X. L. Zha, *Proteomics*, 2007, **7**, 2358-2370.
- 197 H. Zhang, X. J. Li, D. B. Martin and R. Aebersold, *Nat. Biotechnol.*, 2003, **21**, 660-666.
- 40 198 T. Liu, W. J. Qian, M. A. Gritsenko, D. G. Camp II, M. E. Monroe, R. J. Moore and R. D. Smith, *J. Proteome Res.*, 2005, **4**, 2070-2080.
- 199 Y. W. Xu, L. J. Zhang, H. J. Lu and P. Y. Yang, *Proteomics*, 2010, **10**, 1079-1086.
- 45 200 Y. Xu, U. M. Bailey, C. Punyadeera and B. L. Schulz, *Rapid Commun. Mass Spectrom.*, 2014, **28**, 471-482.
- 201 Q. Zhang, N. Tang, J. W. C. Brock, H. M. Mottaz, J. M. Ames, J. W. Baynes, R. D. Smith and T. O. Metz, *J. Proteome Res.*, 2007, **6**, 2323-2330.
- 50 202 M. J. Markuszewski, W. Struck, M. Waszczuk-Jankowska and R. Kaliszan, *Electrophoresis*, 2010, **31**, 2300-2310.
- 203 A. Halama, *Arch. Biochem. Biophys.*, 2014, **564**, 100-109.
- 204 K. Nakano, T. Nakao, K. H. Schram, W. M. Hammargren, T. D. McClure, M. Katz and E. Petersen, *Clin. Chim. Acta*, 1993, **218**, 169-183.
- 55 205 Y. Q. Jiang and Y. F. Ma, *Anal. Chem.*, 2009, **81**, 6474-6480.
- 206 B. Kammerer, A. Frickenschmidt, C. E. Muller, S. Laufer, C. H. Gleiter and H. Liebich, *Anal. Bioanal. Chem.*, 2005, **382**, 1017-1026.
- 60 207 D. Bullinger, R. Fux, G. Nicholson, S. Plontke, C. Belka, S. Laufer, C. H. Gleiter and B. Kammerer, *J. Am. Soc. Mass Spectrom.*, 2008, **19**, 1500-1513.
- 208 R. Tuytten, F. Lemi re, W. V. Dongen, E. Witters, E. L. Esmans, R. P. Newton and E. Dudley, *Anal. Chem.*, 2008, **80**, 1263-1271.
- 65 209 H. P. Jiang, C. B. Qi, J. M. Chu, B. F. Yuan and Y. Q. Feng, *Sci. Rep.*, 2015, **5**, 1-9.
- 210 D. Bullinger, H. Neubauer, T. Fehm, S. Laufer, C. H. Gleiter and B. Kammerer, *BMC Biochem.*, 2007, **8**, 25-38.
- 70 211 E. N. Debruyne and J. R. Delanghe, *Clin. Chim. Acta*, 2008, **395**, 19-26.
- 212 J. E. Shively and J. D. Beatty, *Crit. Rev. Oncol. Hematol.*, 1985, **2**, 100-110.
- 213 Y. F. Wu and S. Q. Liu, *Analyst*, 2009, **134**, 230-235.
- 75 214 X. L. Ma, H. H. Li, M. Wu, C. Sun, L. F. Li and X. D. Yang, *Sensors*, 2009, **9**, 10389-10399.
- 215 J. Ye, Y. Chen and Z. Liu, *Angew. Chem. Int. Ed.*, 2014, **53**, 10386-10389.
- 80 216 G. Schumann, R. Klauke, F. Canalias, S. Bossert-Reuther, P. F. H. Franck, F. J. Gella, P. J. Jorgensen, D. C. Kang, J. M. Lessinger, M. Panteghini and F. Ceriotti, *Clin. Chem. Lab. Med.*, 2011, **49**, 1439-1446.
- 217 A. D. Ellington and J. W. Szostak, *Nature*, 1990, **346**, 818-822.
- 85 218 C. Tuerk and L. Gold, *Science*, 1990, **249**, 505-510.
- 219 H. Y. Nie, Y. Chen, C. C. L  and Z. Liu, *Anal. Chem.*, 2013, **85**, 8277-8283.
- 90